

Strain Measurements
from Deformed Quartz Grains
in Metagreywackes of
the Goldenville Formation,
Meguma Group, Nova Scotia

Strain Measurements from Deformed Quartz Grains
in Metagreywackes of the Goldenville Formation,
Meguma Group, Nova Scotia.

By

Lynn Louise Pryer

A Thesis

Submitted to the Faculty of Science
in Partial Fulfillment of the Requirements
for the Degree
Bachelor of Science

McMaster University

April, 1984

HONOURS BACHELOR OF SCIENCE (1984)
(Geology)

McMASTER
UNIVERSITY

TITLE: Strain Measurements from Deformed Quartz
Grains in the Metagreywackes of the
Goldenville Formation, Meguma Group,
Nova Scotia.

AUTHOR: Lynn Louise Pryer

SUPERVISOR: Dr. P. M. Clifford

NUMBER OF PAGES: ix, 78

Abstract

Metagreywackes of the Goldenville Formation, Nova Scotia, possess a well developed penetrative cleavage. Measurement of strain, based on quartz grain shape, indicates that much of the strain has been achieved by pressure solution of detrital quartz grains. Strain ratios in the system range from $X/Z = 3.8$ in cleavage zones, through 2.0 in intermediate areas, to 1.6 in lithons. The volume lost from cleavage zones ranges from 60 to 70 percent, while loss of volume to the system as a whole is 40 percent or greater. Strain due to plastic deformation is minimal, relative to the strain due to volume loss. The strain within the system is not homogeneous on a centimeter scale, but rather range from low values in mid-lithon zones to much higher values in cleavage zones. Lithon and intermediate areas are representative of the deformation history of the cleavage.

Acknowledgments

I would like to express my gratitude to Dr. P.M. Clifford, for enthusiastically supervising this thesis. I also wish to thank Frank Fueten, Andy Fyon and Jack Henderson for their helpful comments, among other things. Thank you also to Jack Whorwood, for his expert photography, Len Zwicker, for preparing thin sections, and John Kelman, for his assistance with drafting. Finally I would like thank Dave O'Donnell for putting up with me for so long and for helping me get this typed.

TABLE OF CONTENTS

	Page
ABSTRACT	iii
ACKNOWLEDGMENTS	iv
TABLE OF CONTENTS	v
LIST OF FIGURES	vi
LIST OF TABLES	viii
CHAPTER 1	
1.1 Introduction	1
1.2 Geologic Setting	4
1.3 Sample description	7
1.3.1 Cleavage	8
1.3.2 Intermediate	15
1.3.3 Lithons	18
CHAPTER 2	
2.1 Method	21
2.2 Scatter Diagrams	27
2.3 Deformation Plots	52
2.4 Volume Loss	56
2.5 Strain Due to Plastic Deformation	65
2.6 Bulk Strain Estimates	67
2.7 Discussion	69
CHAPTER 3	
Conclusions	72
REFERENCES	74

LIST OF FIGURES

	Page
Figure 1.2.1 Location Map	6
1.3.1 Cleavage G26-415	11
1.3.2 Quartz Grain G26-415	12
1.3.3 G26-415	13
1.3.4 G26-353	14
1.3.5 Intermediate G19-354	17
1.3.6 Lithon G19-354	20
2.1.1 3-D Schematic Fold Section	22
2.1.2 Sketch of Angular Orientation	26
2.2.1 Scatter Diagrams, G26-415	
a) ac section cleavage	32
b) ac section cleavage, 2C	33
c) ac section intermediate	34
d) ac section lithon	34
e) bc section cleavage	35
f) bc section cleavage, 2C	36
g) bc section intermediate	37
h) bc section lithon	37
2.2.2 Scatter Diagrams, G26-353	
a) ac section cleavage	38

b) ac section intermediate	39
c) ac section lithon	39
d) bc section cleavage	40
e) bc section intermediate	41
f) bc section lithon	41
2.2.3 Scatter Diagrams, G19-354	
a) ac section cleavage	42
b) ac section intermediate	43
c) ac section lithon	43
d) bc section cleavage	44
e) bc section intermediate	45
f) bc section lithon	45
2.2.4 Scatter Diagrams, G20-747	
a) ac section cleavage	46
b) ac section intermediate	47
c) ac section lithon	47
2.2.5 Scatter Diagrams, G20-753	
a) ac section cleavage	48
b) ac section intermediate	49
c) ac section lithon	49
d) bc section cleavage	50
e) bc section intermediate	51
f) bc section lithon	51
2.3.1 Deformation Plot	55

2.4.1 Deformation Plot with Volume Loss	57
2.4.2 Sketch of Change in Deformation	
Path	64

LIST OF TABLES

	Page
Table 1 Calculated Strain Values	28
2 Calculated Volume Loss	58
3 Strain Due to Plastic Deformation	66

Chapter 1

1.1 Introduction

The origin and significance of pressure solution cleavage is currently one of the most active topics in structural geology. The effects of pressure in sedimentary rocks was first recognized by Sorby in 1863. He later named the process "Pressure Solution" in 1908. Since then this process has been called upon to explain many compaction and deformation features in sedimentary and metamorphic rocks.

The importance of pressure solution in the formation of cleavage in phyllosilicate-bearing sandstones has recently been dealt with by many authors including Williams (1972), Lisle (1977), Mitra (1978), Beach (1979,1982), Fry (1981), Woodland (1982), and Onasch (1983). During the cleavage forming process, quartz grains are "pressure" dissolved and removed from the local system resulting in a concentration of phyllosilicates. Whether the actual growth of

phyllosilicate occurs within the cleavage domain by inward chemical transfer of material from outside the local system is not yet resolved.

The determination of strain in mildly deformed greywackes can be done based on the shape of quartz grains. Three factors contribute to the variation in the shapes and orientations of deformed particles. These are 1) initial grain shape, 2) initial grain orientation and 3) strain heterogeneity. Errors in measurement also play a role in the final analysis.

Details of methods of strain computation have been discussed by Ramsay (1967), Dunnet (1969) and Elliot (1970). Strain is generally regarded as being homogeneous within the scale of the sample.

It is the aim of this study to quantify the finite strain experienced by a set of metagreywacke samples possessing a well developed pressure solution cleavage. In order to determine the bulk strain of the system, samples have been divided into three regions, based on grain shape and mica concentrations, so that homogeneous strains may be assumed.

From the determination of strain in three dimensions it is possible to quantify the volume lost from the system (Ramsay, 1967; Ramsay and Wood, 1972). By doing so, it is

hoped that the extent to which pressure solution plays a role in cleavage formation can be demonstrated.

1.2 Geologic Setting

The Meguma Group is divided into two formations, the underlying, quartz-arenite-rich Goldenville Formation and the overlying slate-rich Halifax Formation. The Meguma Group occupies a major portion of southwest Nova Scotia.

The Goldenville Formation consists of metagreywacke and interbedded slate. Thickness and number of slate interbeds generally increase towards the top of the formation. Primary structures seen include: graded bedding, cross bedding, flute marks, grooves, ball and pillow, ripple marks, scour and fill and sand volcanoes. Primary structures along with bedding sequences suggest that deposition was largely via turbidity current, (Phinny, 1961; Schenk, 1970).

The Halifax Formation consists of thinly laminated black and grey slates with minor interbedded meta-siltstone and meta-argillite. The boundary between these formations appears to be conformable.

The metagreywackes of the Goldenville Formation are composed mainly of detrital quartz grains which can account for as much as 75 percent of a unit. The remainder consists of feldspar, rock fragments and micas.

Samples used were located in the Goldenville anticline,

Goldenville, Nova Scotia, (Figure 1.2.1). This anticline is one of many occurring in the Meguma Group. Folds are doubly plunging and major fold axial traces trend roughly east to west. Metagreywacke beds exhibit a penetrative cleavage which is often anastomosing. Slate beds possess well developed slaty cleavage. In anticlines, the greywacke cleavage forms a convergent fan about the fold axial surface, (Ramsay, 1967; page 405, figure 8), while the slaty cleavage forms a divergent fan.

The metamorphic grade of the area increases northward from lower greenschist at the coast to staurolite grade in the north just south of the St. Mary's Fault. The folding and metamorphism of the Meguma sediments occurred during the Acadian Orogeny, but detrital muscovite has been dated at 487 +/- 29 million years, (Poole, 1971), making the Formation of Cambro-Ordovician age.

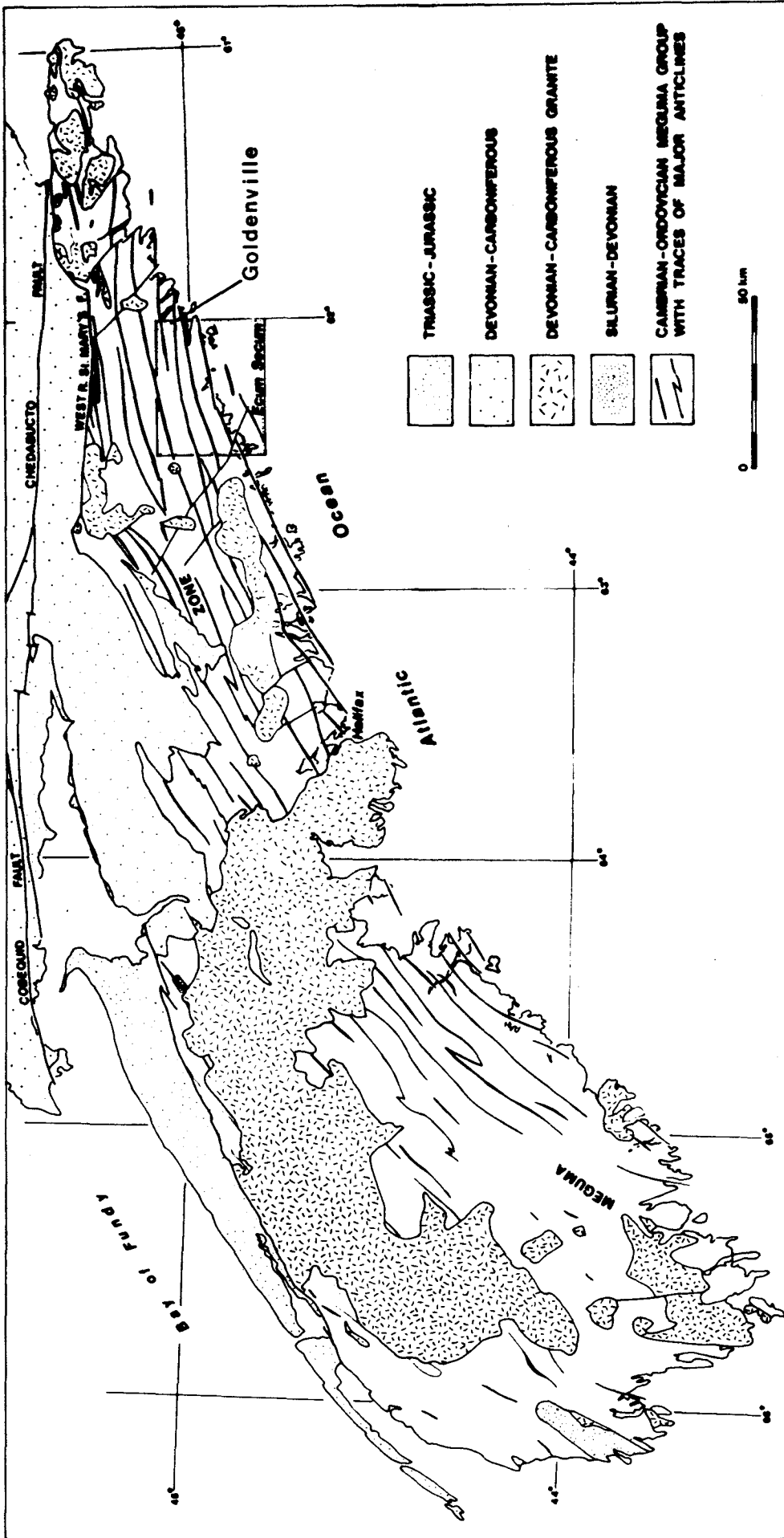


Figure 1.2.1. Location Map.

1.3 Sample Description

Samples used were supplied from drill cores of the Goldenville anticline, Goldenville, Nova Scotia, courtesy of Barry Jones, Goldenville Exploration LTD.. All samples used were recovered from a depth of 100m or more so that surface weathering would not present a problem.

The metagreywacke beds (Bouma A units) display a persistent and well developed spaced cleavage which trends E-W. Samples studied are from the north limb and core of the anticline. No samples from the vertical to overturned south limb have been used, mainly because the cleavage is not as well developed there. The original sedimentary fabric appears to have been random, based on the symmetry of orientation diagrams, which is to be expected in a Bouma A unit.

The overall composition is 68% quartz, 28% mica, with the remaining 4% being feldspar, carbonates and opaques. Each section has been divided into three domains based on grain shape and phyllosilicate concentration: cleavage, intermediate and lithon.

1.3.1 Cleavage

The cleavage is composed mainly of preferentially oriented white mica flakes, which concentrate in planar regions and essentially define the cleavage orientation (Figure 1.3.1). Also found within the cleavage planes are partially pressure dissolved detrital quartz grains. The grains are rectangular to lens shaped with their long axes being parallel to subparallel to the cleavage orientation (Figure 1.3.2). These grains may possess quartz beards, but beards contribute a negligible amount to the total quartz in the cleavage. Most grains do possess mica beards. Minor constituents within cleavage zones include feldspar, chlorite, biotite and opaques. Feldspar grains, when seen within cleavage zones, also tend to be rectangular in shape but their aspect ratios are lower than those seen in the quartz grains.

The extent of cleavage development varies between samples. The boundaries of cleavage zones vary from abrupt to gradational into the intervening lithon. Generally those samples possessing very well defined, wide cleavage will have the more abrupt boundaries, (Figures 1.3.3 and 1.3.4). Gradational boundaries are seen where the cleavage plane is bounded on either side by an intermediate area (discussed

below). Width of cleavage zones ranges between 0.2mm and 3.0mm. Cleavage spacing normally varies between 5mm and 10mm, the average spacing being 8mm.

Cleavage zones contain substantially less quartz than other areas within the sample. They also contain a much higher proportion of micas, which can account for 35% to 65% of the cleavage volume.

The length of quartz grains within the cleavage range from 55 micrometers to 8 micrometers and widths from 20 micrometers down to 1 micrometer or less. Anything smaller than 1 micrometer could not be measured due to inaccuracy of measurement at that scale.

Across the width of a thin section, variations in the cleavage plane orientation are within +/- 5 degrees of the mean cleavage orientation. On a larger scale cleavage may bifurcate or anastomose (Figures 1.3.3 and 1.3.4). The amount of fluctuation in the cleavage orientation is crudely related to the extent of cleavage development. The very well developed cleavage planes have a much smaller fluctuation in orientation and possess small splays rather than bifurcations.

On the scale over which individual sets of measurements were taken the variation in cleavage orientation was less than 5 degrees. Because of this cleavage zones can be considered to be rectiplanar.

The overall character of the cleavage is identical in mutually perpendicular sections cut normal to the cleavage plane. The average length of quartz grains and their shapes in these sections are essentially identical as well.

Figure 1.3.1 Cleavage from slide G26-415BC. Note the concentration of phyllosilicates. Cleavage boundaries can be seen with adjacent intermediate zones. Compare the rectangular grain within the cleavage to the rounded grain immediately adjacent to the cleavage. The length of the square grain is 0.7 mm.



Figure 1.3.2 Slide G26-415BC. Rectangular quartz grain within a cleavage zone. The rectangular shape is due to unidirectional pressure solution. Note the mica beards at the ends of the grain. The grain is 0.5 mm.

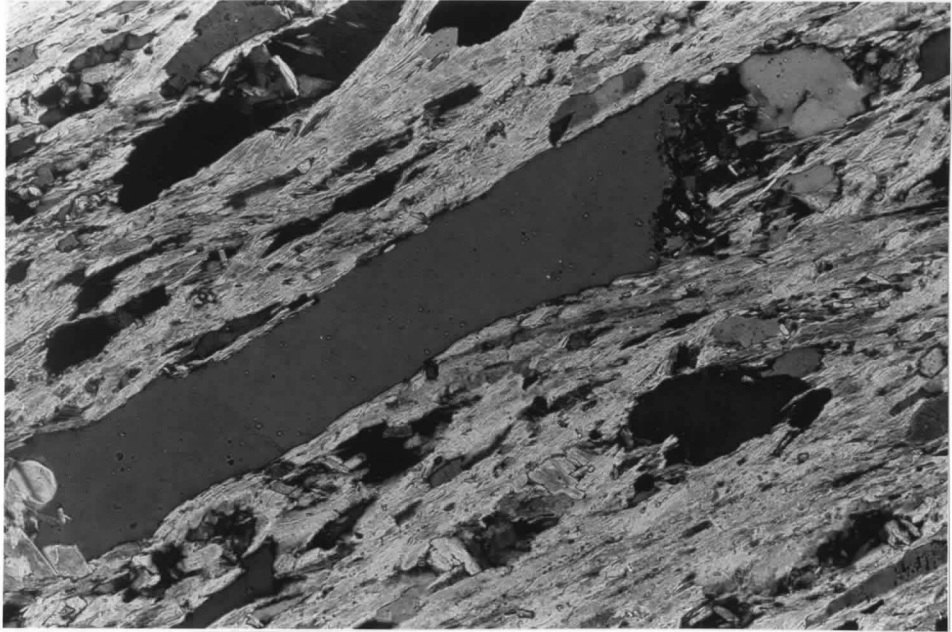


Figure 1.3.3 Slide G26-415AC. Cleavage zones are well defined and are generally linear or anastomosing. An "island" occurs within the wide cleavage band defined by an increased concentration of quartz grains. The width of the photograph is 2.2 cm.

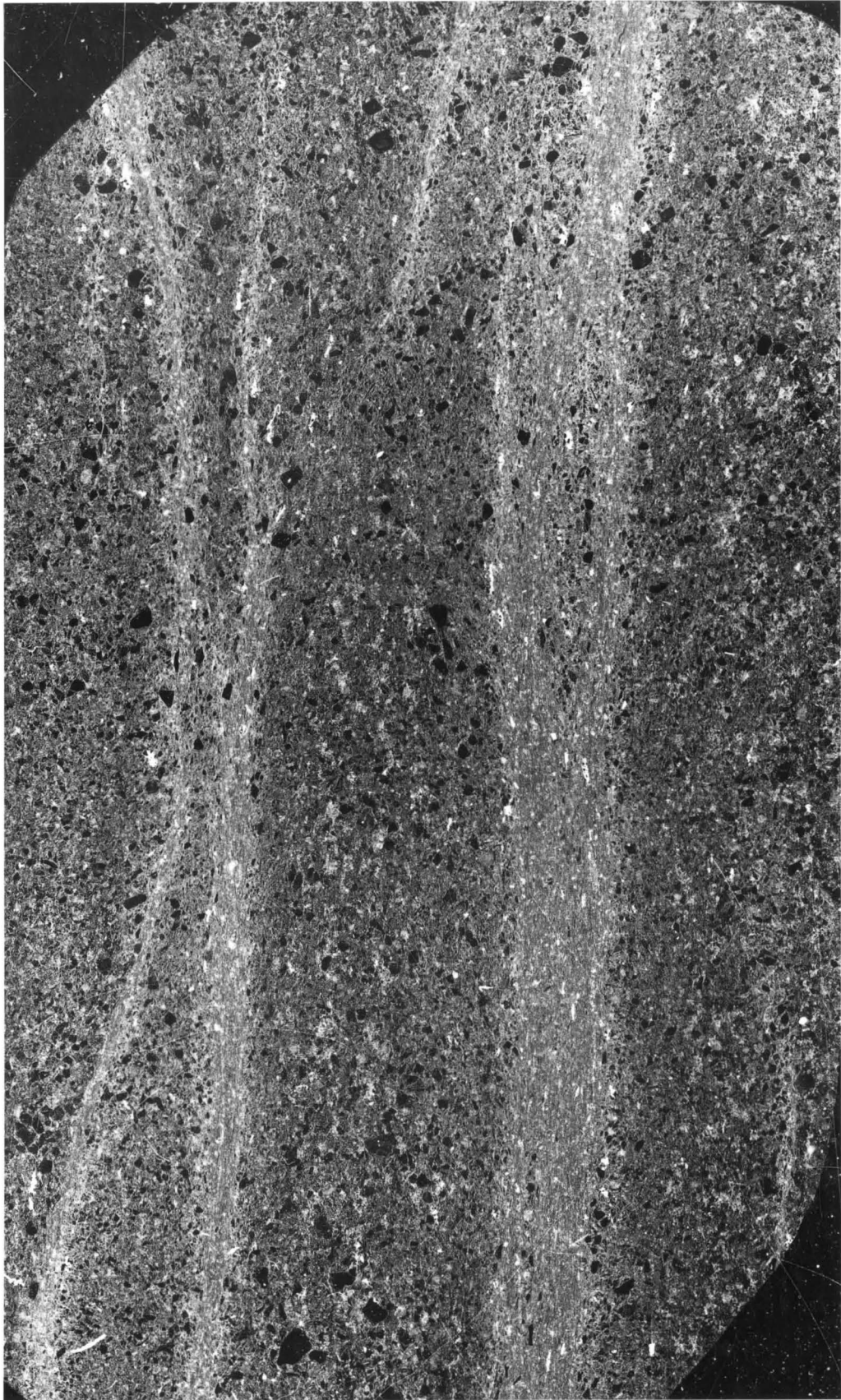
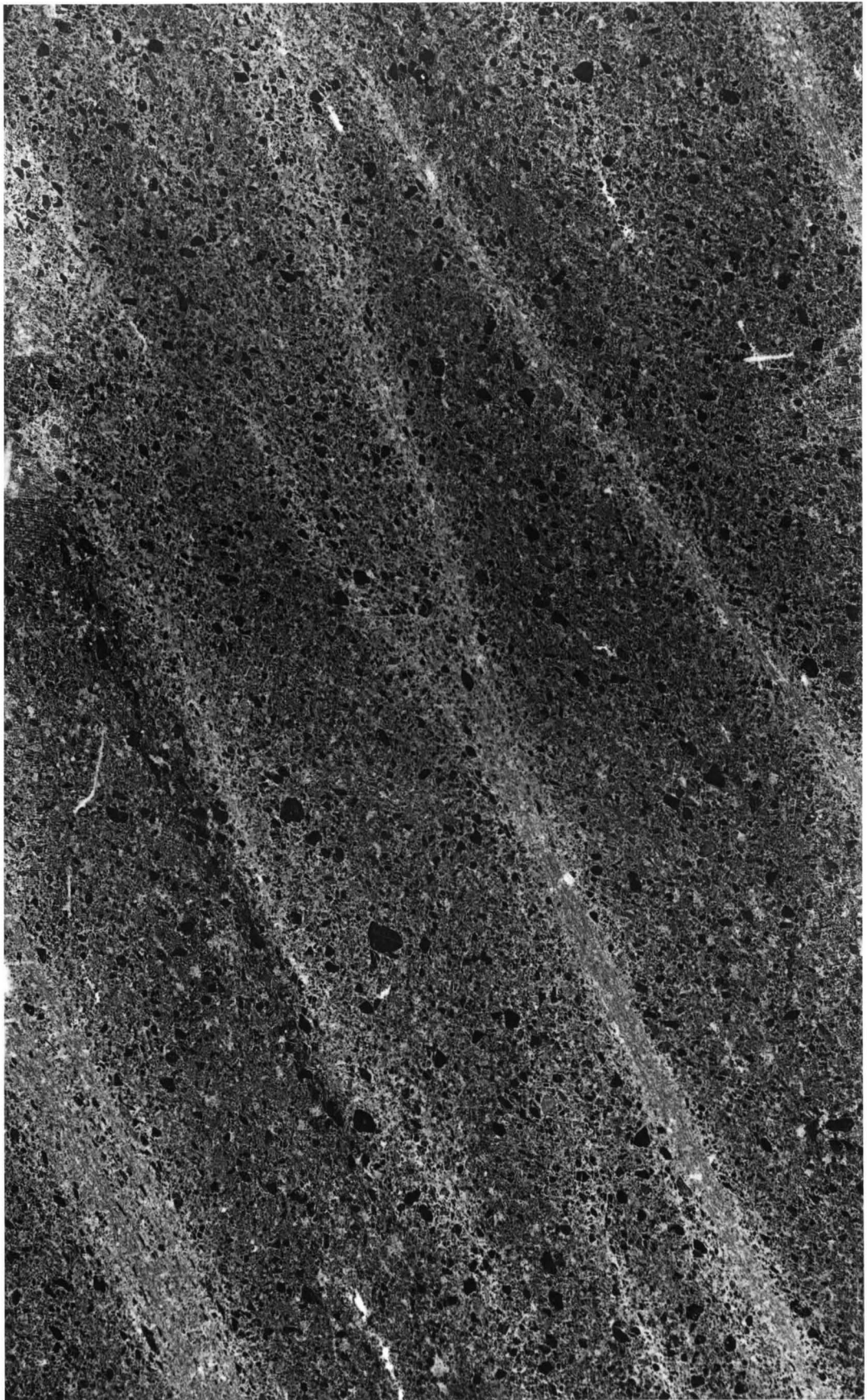


Figure 1.3.4 Slide G26-353AC. Cleavage zones in this slide are less well defined. Cleavage zones are linear but the orientation is variable. Note the bifurcation in the cleavage in the center of the photograph. The width of the photograph is 1.5 cm.



1.3.2 Intermediate Areas.

Intermediate areas have been defined here as those areas possessing a well developed grain cleavage (see figure 1.3.5). Quartz grains in these areas account for 50% or more of the volume. Quartz grains are predominantly eye shaped with the tapered ends defining the grain cleavage orientation. This orientation, although less well defined than the cleavage zones, is parallel to the cleavage plane. Micas in this zone bend (curve) around the neighboring quartz grains, which essentially control the orientation of the micas.

Intermediate areas are found in three locations relative to the cleavage:

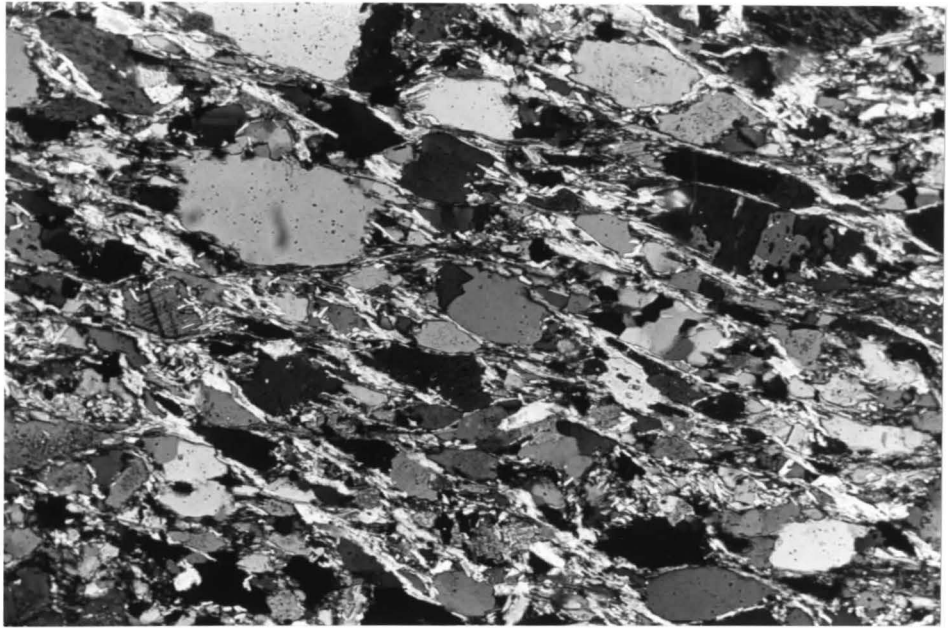
- 1) as islands within a cleavage zone (see figure 1.3.4). In this case they are localized areas with a high concentration of quartz grains, within a cleavage plane. These areas result from the coalescence of neighboring anastomosing cleavage zones.
- 2) immediately adjacent to cleavage zones. This is the most common position. The transition from cleavage to intermediate may be abrupt or gradational, depending on the extent of cleavage development.
- 3) within lithon areas located between two cleavage planes.

The width of lithons containing these "planes" is generally larger than average. These areas might be considered a "failed" cleavage, or a poorly developed cleavage.

The percent mica within intermediate areas is intermediate to that found in the cleavage and lithon areas. The same can be said for the percent quartz.

The width of intermediate areas may vary from 1 mm to 5 mm.

Figure 1.3.5 Intermediate area from slide G19-354AC.
Quartz grains are eye shaped and have a strong preferential orientation. Mica orientations are controlled by neighbouring quartz grains. The width of the photograph is 3 mm.



1.3.3 Lithons

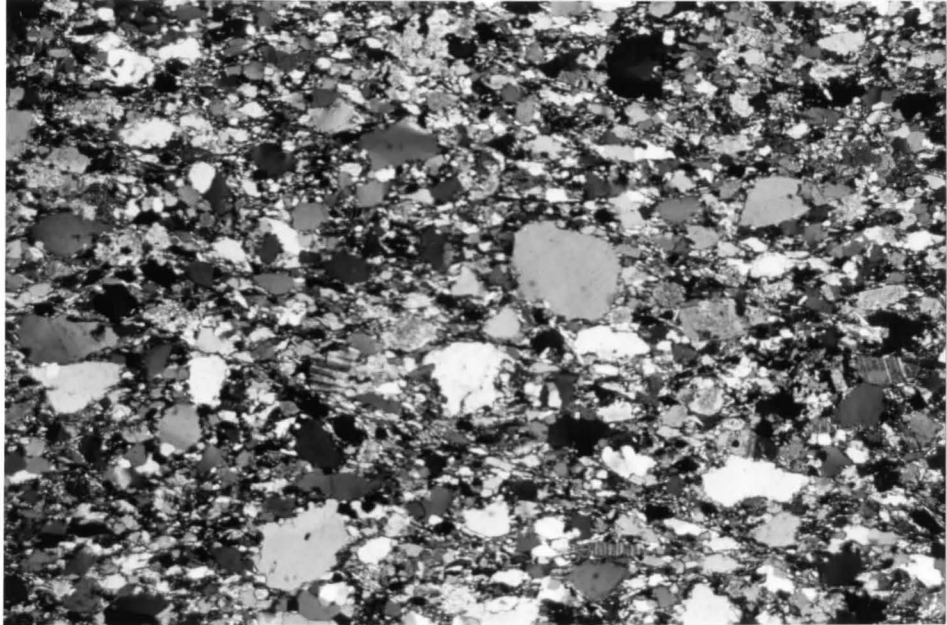
The lithons are those areas between cleavage zones which have undergone the least amount of apparent deformation. They are composed of 60 to 80 percent detrital quartz grains, the size and shape of these grains being highly variable (Figure 1.3.6). Grain sizes range from 500 micrometers down to 1 micrometer. Axial ratios in the lithons are low compared to those in cleavage and intermediate areas, and grain shapes range from angular to subrounded. Other constituents found in the lithons include white and dark micas, which account for 10 to 20 percent of the volume, as well as carbonate, feldspar and opaques. Grain boundaries tend to be sutured and most grains show a faint undulatory extinction. The extent of recrystallization within lithons varies between samples. In all cases, recrystallized grains were avoided during measurement. Many of these grains appear to have been detrital quartzite fragments, containing small inclusions of clay particles and having a well defined clast outline.

The quartz grains in the lithons possess a very weak preferred orientation which is always within +/- 5 degrees of the measured cleavage orientation. This fabric only becomes apparent after measurements of long axis

orientations have been done.

Only approximately 5 percent of the quartz grains possess quartz beards, (which are generally minor), but most grains have mica beards. These micas are oriented essentially parallel to the cleavage orientation. The overall mica orientation in the lithons is equivalent to that in the cleavage, but is not so well developed.

Figure 1.3.6 Lithon area from slide G19-354AC. Grains do not show a strong preferential orientation. Some subgraining can be seen. The width of the photograph is 3 mm.

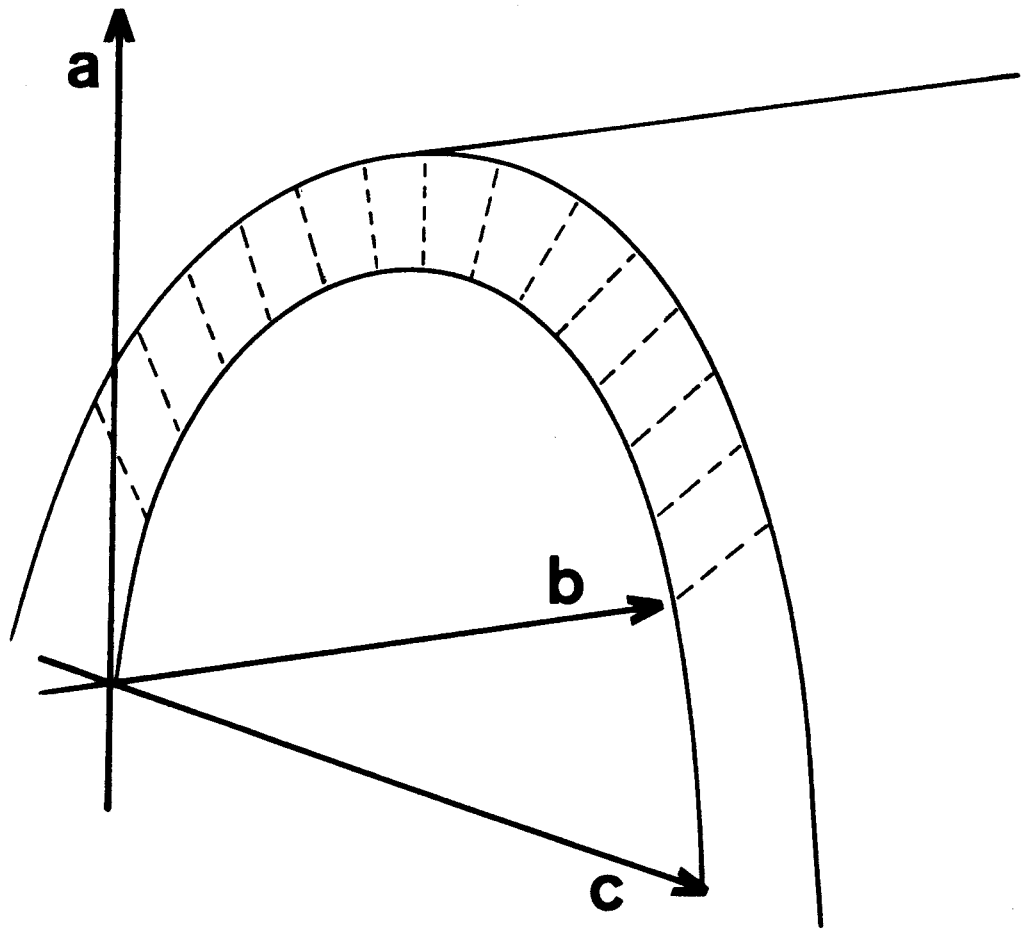


CHAPTER 2

2.1 Method

A lineation is developed in the cleavage planes. In the field this lineation is horizontal. Core was oriented based on this lineation. The cleavage plane is assumed to be equivalent to the X Y principal plane (Ramsay & Wood, 1972; Dunnet, 1969). The ac sections (Figure 2.1.1) were cut normal to both the lineation and the cleavage plane. These sections correspond to the X (or Y) Z principal plane. A second section was then cut normal to both the ac section and the cleavage plane. These sections correspond to the Y (or X) Z principal plane. Where cleavage is vertical, ie. in samples at or near the fold core, this second section is equivalent to a bc section. In samples derived from farther down the limb the cleavage is no longer vertical, so this second section would correspond to a plane intermediate between the bc and ab planes. Error in orientation and sectioning has been assumed to be less than 5 degrees.

Figure 2.1.1 Diagrammatic representation of an anticline showing orientations. Cleavage is shown forming a convergent fan.



Thin sections were then placed on a Shadowmaster and enlarged on a screen by 100 times. A reference axis was arbitrarily chosen against which grain orientations could be measured (Figure 2.1.2). Each grain was oriented with its long axis parallel to the EW screen border by rotating the stage. The length (X) and width (Y) of each grain was measured and its orientation (θ) was read directly off the stage. Measurements were taken in three different areas in each section i.e. cleavage, intermediate, and lithon, as defined above. In each area between 50 and 105 detrital quartz grains were measured. (Dunnet (1969) suggested that 50 to 60 particles are necessary to define tectonic strain values in conglomerate and grit specimens, for results to be reproducible). Quartz beards, when they occurred, were not measured as part of the grain. The size of particles measured ranged from 500 micrometers to 1 micrometer. For grains possessing a low axial ratio, error arises in defining the orientation of long axes, since the long axis itself is hard to define. The accuracy of measurement was ± 0.5 micrometers, and hence, very small grains have a much larger proportionate error than larger grains. In the cleavage zones it is not uncommon to find long, ribbon shaped grains having a width on the order of 1 micrometer, so the error in the axial ratio of these grains may be substantial. Because of this, these grains were avoided

wherever possible.

The axial ratio of each grain was calculated and plotted against the long axis orientation on a standard $A\langle T \rangle$ vs θ (Ramsay type) diagram. The axis of symmetry was determined using $(A\langle T \rangle - 1)$ weighted vector summation i.e.

$$\bar{\theta} = \text{Arctan} \left(\frac{\sum_{n=0}^i n_i \cos \theta}{\sum_{n=0}^i n_i \sin \theta} \right)$$

Where: θ = long axis orientation

$\bar{\theta}$ = mean azimuth

n_i = $A\langle T \rangle - 1$

$A\langle T \rangle$ = axial ratio

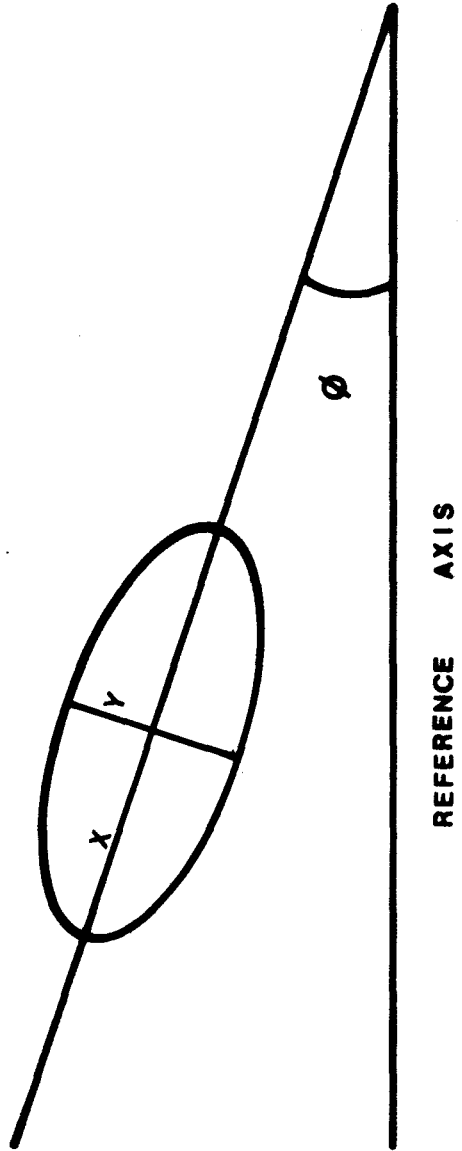
The $(A\langle T \rangle - 1)$ weighted vector mean is used because particles having an axial ratio of one should not have any weight on the mean orientation (Hsu, 1971). This also decreases the effective error in orientation due to particles having a low axial ratio.

The tectonic strain $(A\langle t \rangle)$ was determined by taking the logarithmic mean of the $A\langle t \rangle$ values. The reciprocal values of ratios for points lying at an angle of $\theta = 45$ degrees were used in the calculation $(1/A\langle T \rangle)$ so that the total scatter on a logarithmic $A\langle T \rangle$ axis would be symmetrical about the strain value (Dunnet 1969).

The theoretical curves of varying initial ratios $(A\langle o \rangle)$

were calculated using the strain values determined for each section. These curves were also plotted on the $A\langle T \rangle$ vs θ diagram. Since the plots are essentially symmetric about the $\theta = 0$ axis, points with negative θ values have been reflected across the $\theta = 0$ axis.

Figure 2.1.2 Sketch showing grain orientation and long
(X) and short (Y) axes



2.2 Scatter Diagrams: $A\langle T \rangle$ vs θ

The method used to determine strain values is that of Dunnet (1969), which does not differ significantly from that outlined by Ramsay (1967). In the diagrams $A\langle T \rangle$ (equivalent to $\sqrt{R\langle T \rangle} = X/Y$ in Ramsay) is plotted on the ordinate and θ , azimuth or long axis orientation, is plotted on the abscissa. The scatter diagrams for all the sets of measurements are shown in figures 2.2.1 to 2.2.5. The shape of each plot clearly illustrates the extent to which the section has been strained. Those sections having the smallest fluctuation in orientation are those measured in the cleavage zones. The fluctuation angle increases from cleavage through intermediate to lithon areas. As well as the increase in fluctuation, the maximum $A\langle T \rangle$ value measured decreases from cleavage to lithon. The calculated strain values for each section are listed in Table 1. Values for X (or Y)/ Z are given for both ac and bc sections. The average strain values decrease from 3.8 in the cleavage, through 2.0 in the intermediate area to 1.6 in the lithon.

It is apparent from these values that the principal strain axis (X) alternates randomly between the ac and bc sections. The common axis in these sections (c axis) corresponds to the Z principal strain direction. From this,

TABLE 1

Calculated Strain Values

Sample	A<t>(ac)	A<t>(bc)	Strain Ratio
G26-353			
C	4.01	3.70	1.08:1:0.27
I	1.86	1.80	1.03:1:0.56
L	1.49	1.42	1.05:1:0.70
G26-415			
C	4.64	4.02	1.15:1:0.25
2C	4.06	3.58	1.13:1:0.28
I	1.87	2.45	1.31:1:0.53
L	1.23	1.60	1.30:1:0.81
G20-747*			
C	3.60		
I	2.13		
L	1.32		
G20-753			
C	3.02	3.85	1.27:1:0.33
I	2.04	1.77	1.15:1:0.56
L	1.25	1.29	1.03:1:0.80
G19-354			
C	3.34	3.57	1.07:1:0.30
I	2.23	2.20	1.01:1:0.45
L	1.45	1.41	1.03:1:0.71

C Cleavage; I Intermediate; L Lithon.

* No bc section was available.

the shape of the strain ellipsoid is considered to be a uniaxial oblate ellipsoid (Ramsay, 1967; pg.137) in which the cleavage plane holds the X and Y principal strain directions. The increase in fluctuation angle and the decrease in strain ratios from cleavage to lithon indicates that the strain, on the scale of a few centimeters, is heterogeneous. The values also suggest that the strain decreases exponentially from cleavage to lithon.

If the lithon is considered to represent the original rock, prior to deformation, then the intermediate zones appear to represent the intermediate step in cleavage formation. This observation is also supported by the morphology and location of intermediate zones within each section. Where cleavage zones terminate, the position occupied by the cleavage plane is replaced by an intermediate zone which, in turn, is replaced by lithon. This change from a well developed cleavage into lithon morphology is gradational (ie. cleavage tapers out).

Also plotted on the diagrams are the theoretical curves which correspond to the calculated strain value in each section. The theoretical curves were calculated using the equation developed by Dunnet(1969):

$$\cos 2\theta = \frac{A\langle o \rangle (A\langle t \rangle^2 + 1)(A\langle T \rangle^2 + 1) - 2A\langle t \rangle A\langle T \rangle (A\langle o \rangle^2 + 1)}{A\langle o \rangle (A\langle t \rangle^2 + 1)(A\langle T \rangle^2 + 1)}$$

Where θ = fluctuation angle after deformation

θ = original (undeformed) orientation

$A\langle o \rangle$ = initial axial ratio

$A\langle T \rangle$ = final axial ratio

$A\langle t \rangle$ = axial ratio of the strain ellipse

Each curve was calculated for values of:

$\theta = 0, 15, 30, 45, 60, 75, 90$.

The $a\langle t \rangle$ used was the strain ratio for the particular section and one curve was calculated for each of:

$A\langle o \rangle = 1.5, 2.0, 2.5, \text{ and } 3.0$.

If less than two points fell outside of any particular curve, the curve for the next highest initial ratio was not plotted.

This equation assumes that strain is homogeneous, but not necessarily one of constant volume. It considers the homogeneous deformation of an ellipse of one particular initial ratio being strained to a particular finite value. The strain ratio is the final axial ratio of an originally circular particle undergoing the same amount of strain.

The fit of the curves to the measured points in the

cleavage and intermediate areas is amazingly close. This closeness of fit strongly suggests that, on a millimeter scale the strain is homogeneous. The fit of the curves in the lithons is not quite so close, but at such low strain values in a natural system it is not surprising to find relatively large deviations from ideality.

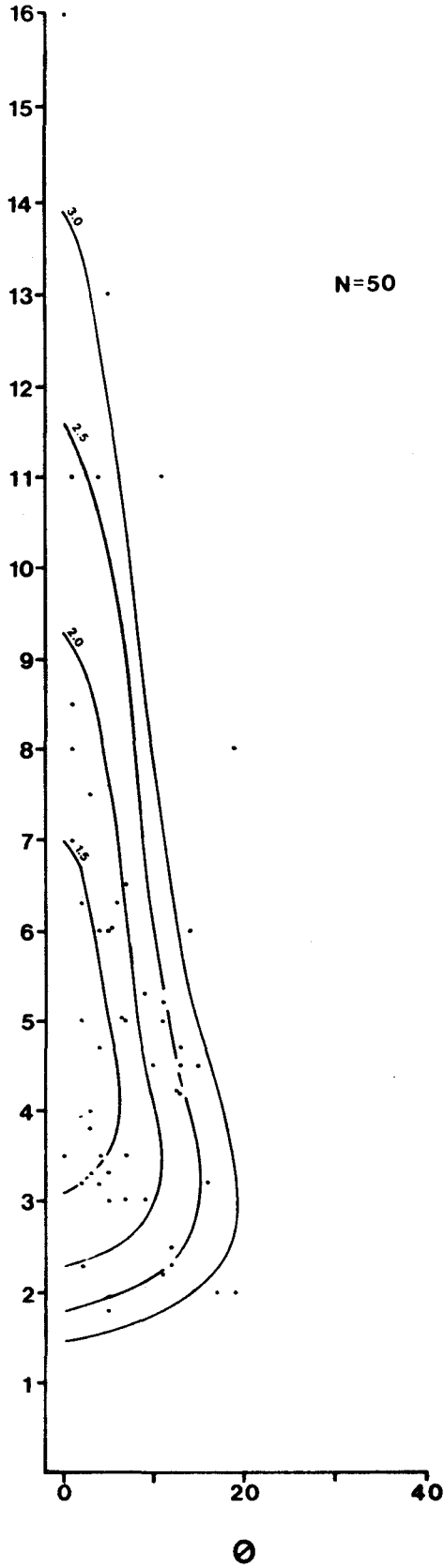
The initial ratio of grains in all sections essentially falls between $A\langle o \rangle = 1.0$ and $A\langle o \rangle = 3.0$, with the majority of points falling below $A\langle o \rangle = 2.0$. Since the average axial ratio for natural detrital quartz grains is approximately 1.5, (Griffiths, 1967), and is essentially independent of source, these values are not unrealistic.

Figure 2.2.1a-h Scatter diagrams for slide G26-415

(a)

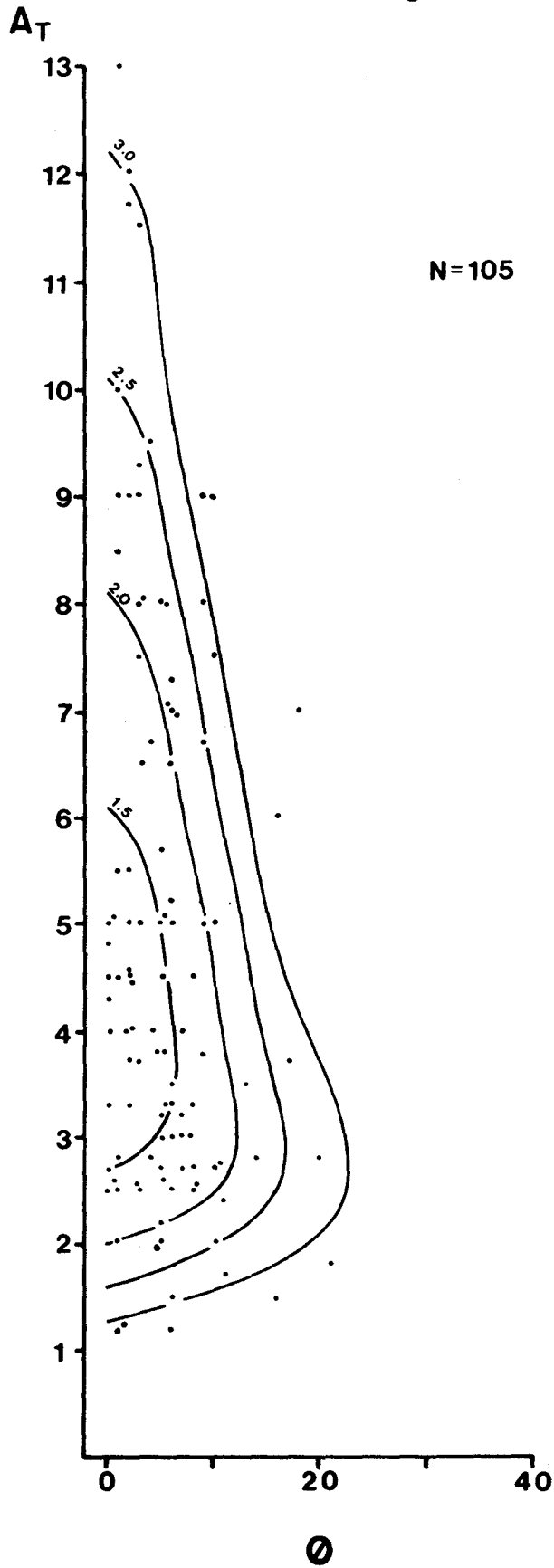
G26-415-AC
Cleavage

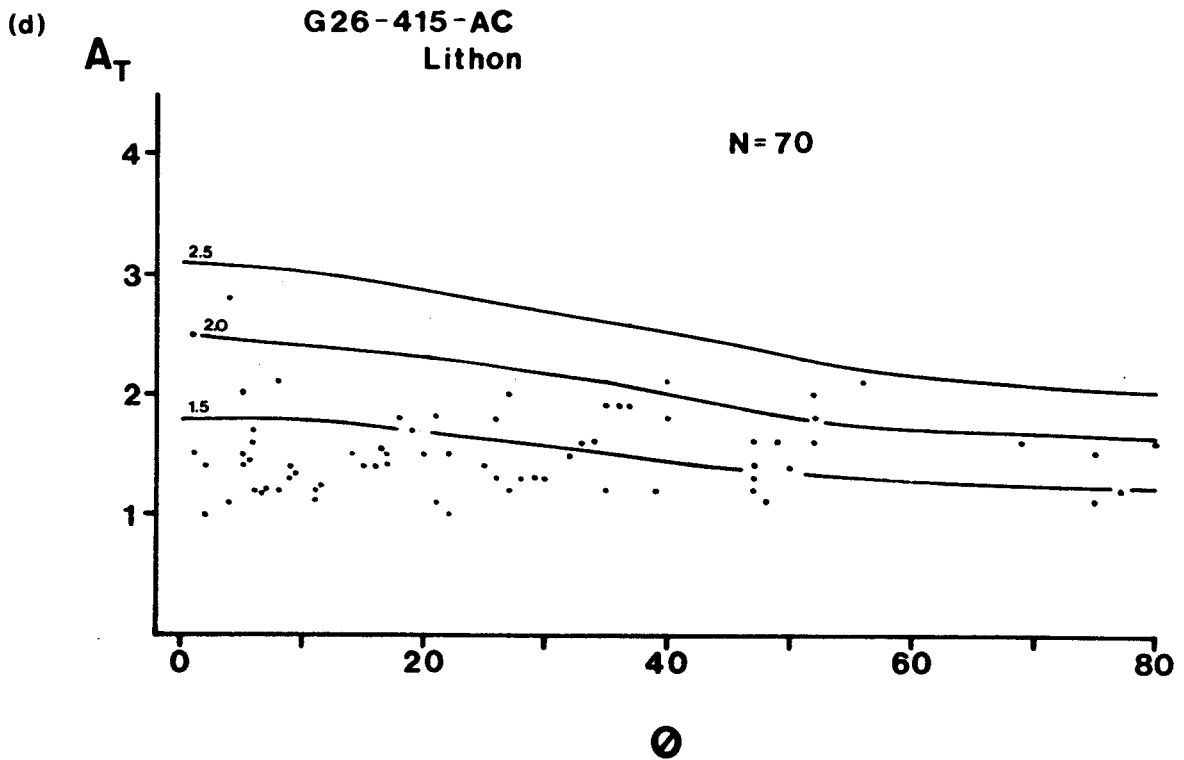
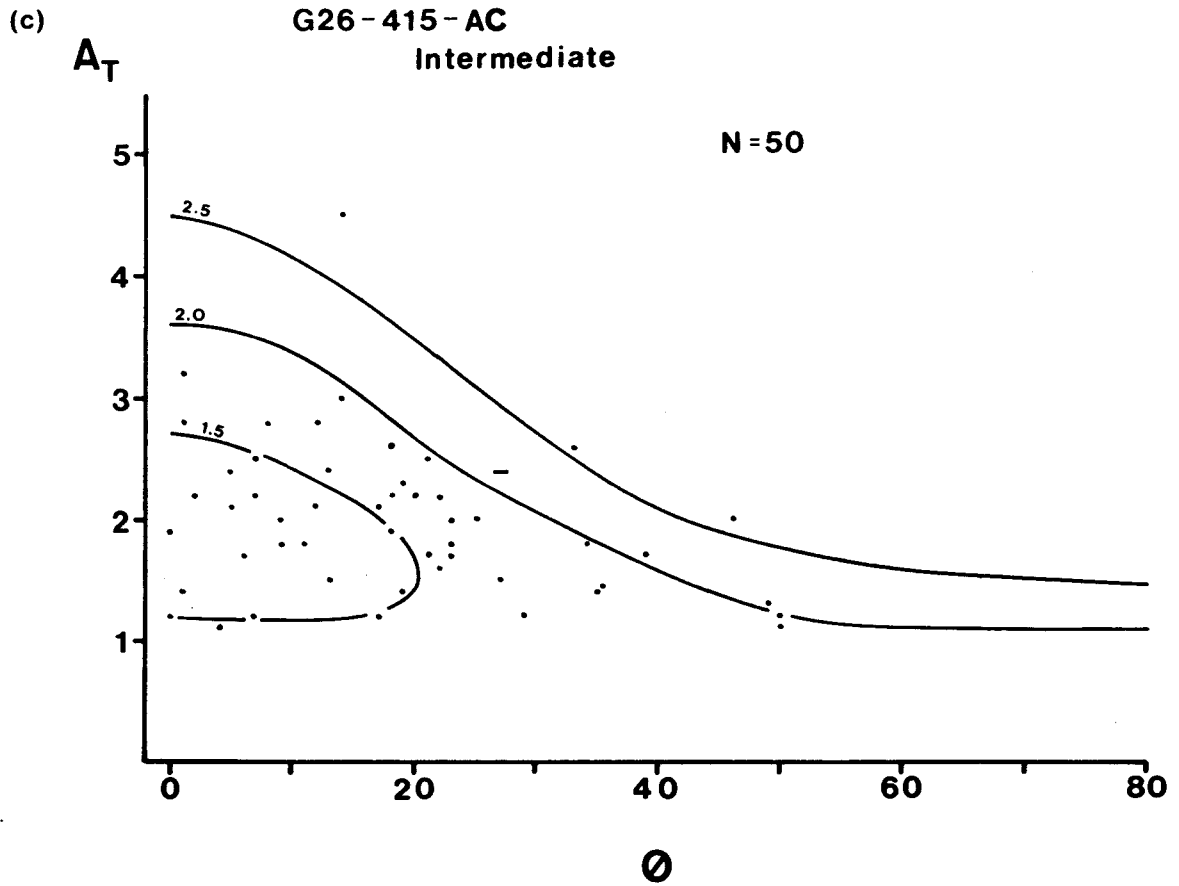
A_T



G26-415-AC-2C
Cleavage

(b)

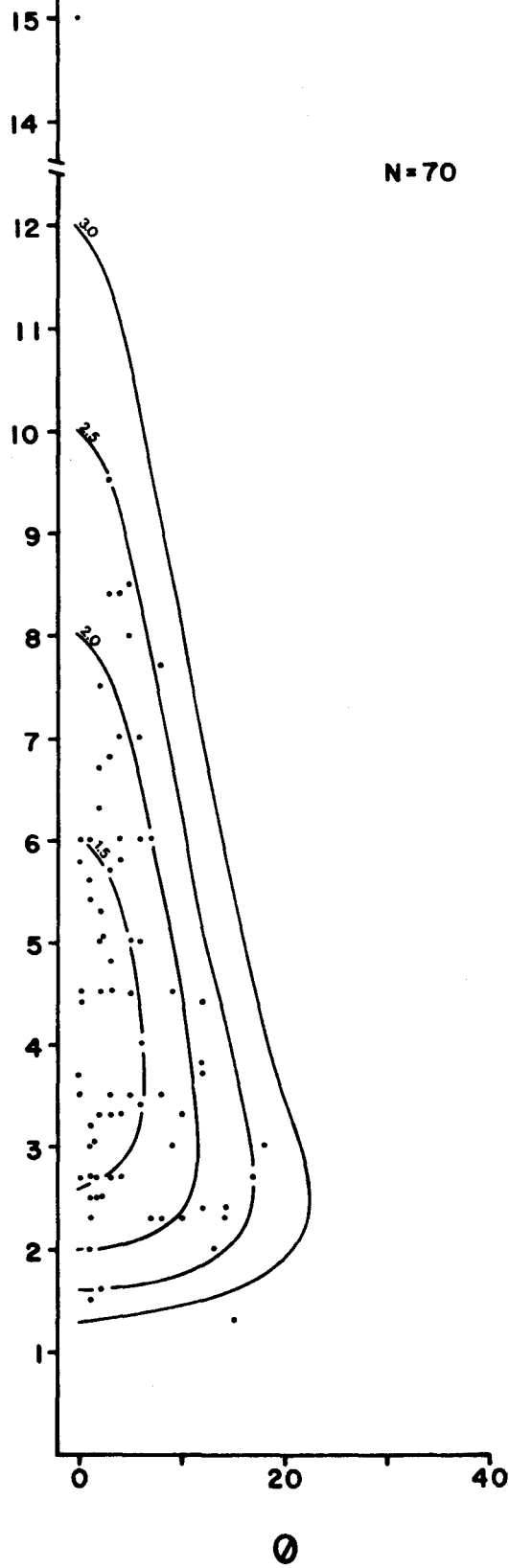




(e)

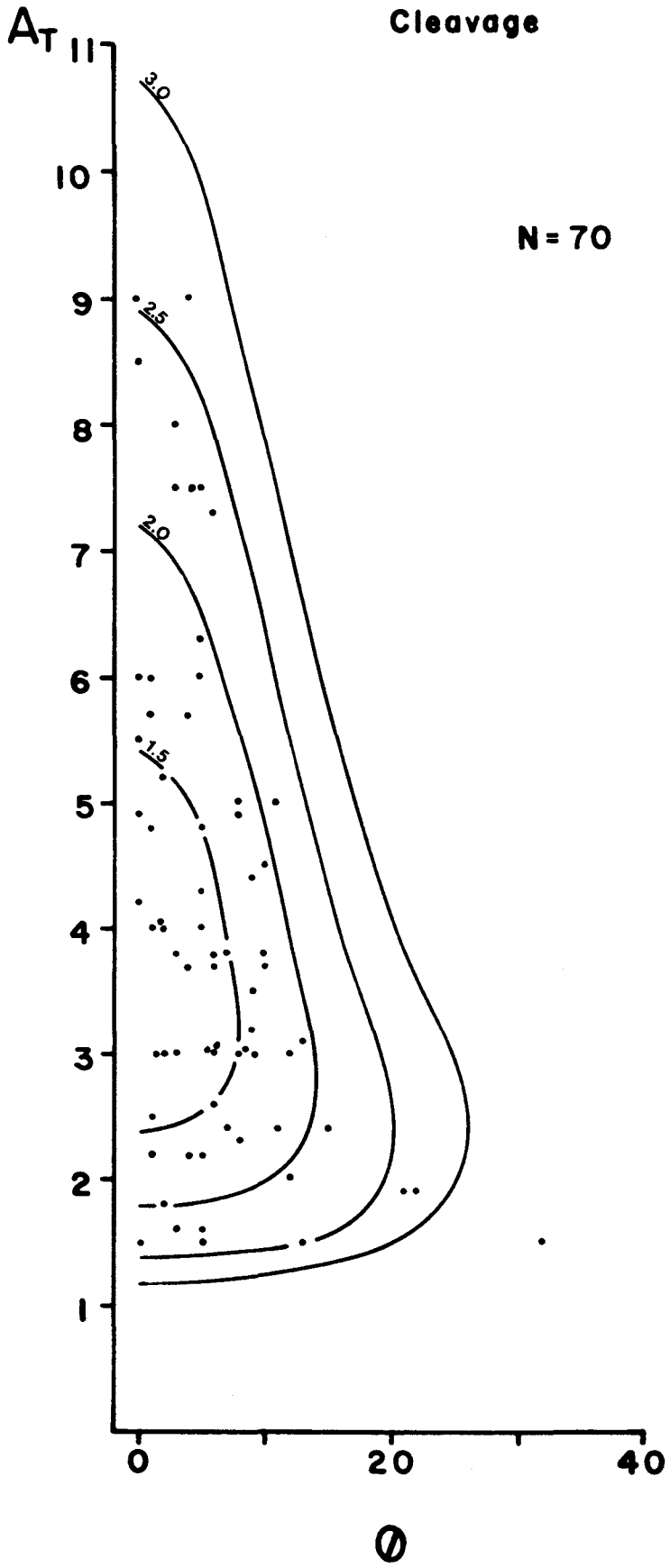
G26-415-BC
Cleavage

A_T

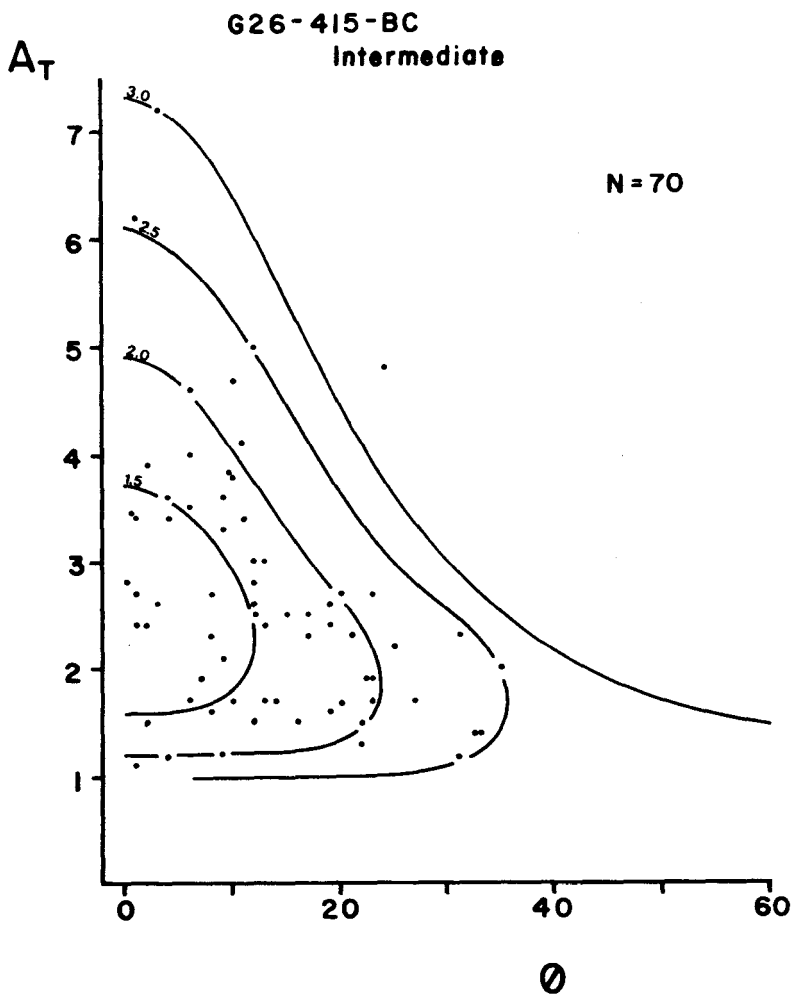


(f)

G26-415-BC-2C
Cleavage



(g)



(h)

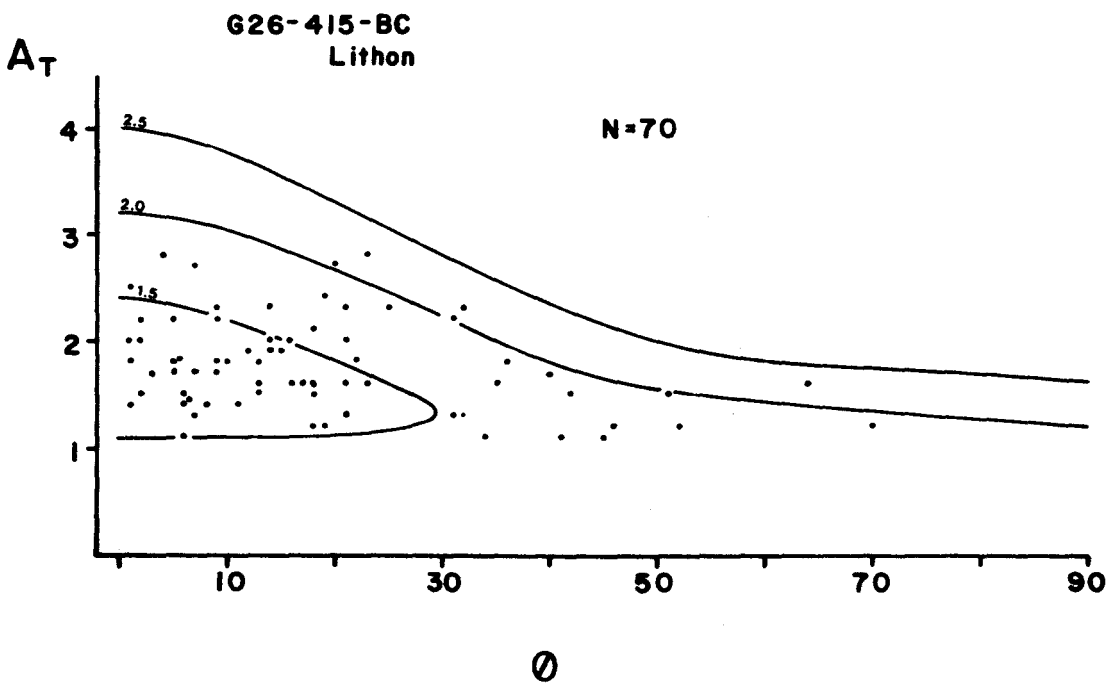
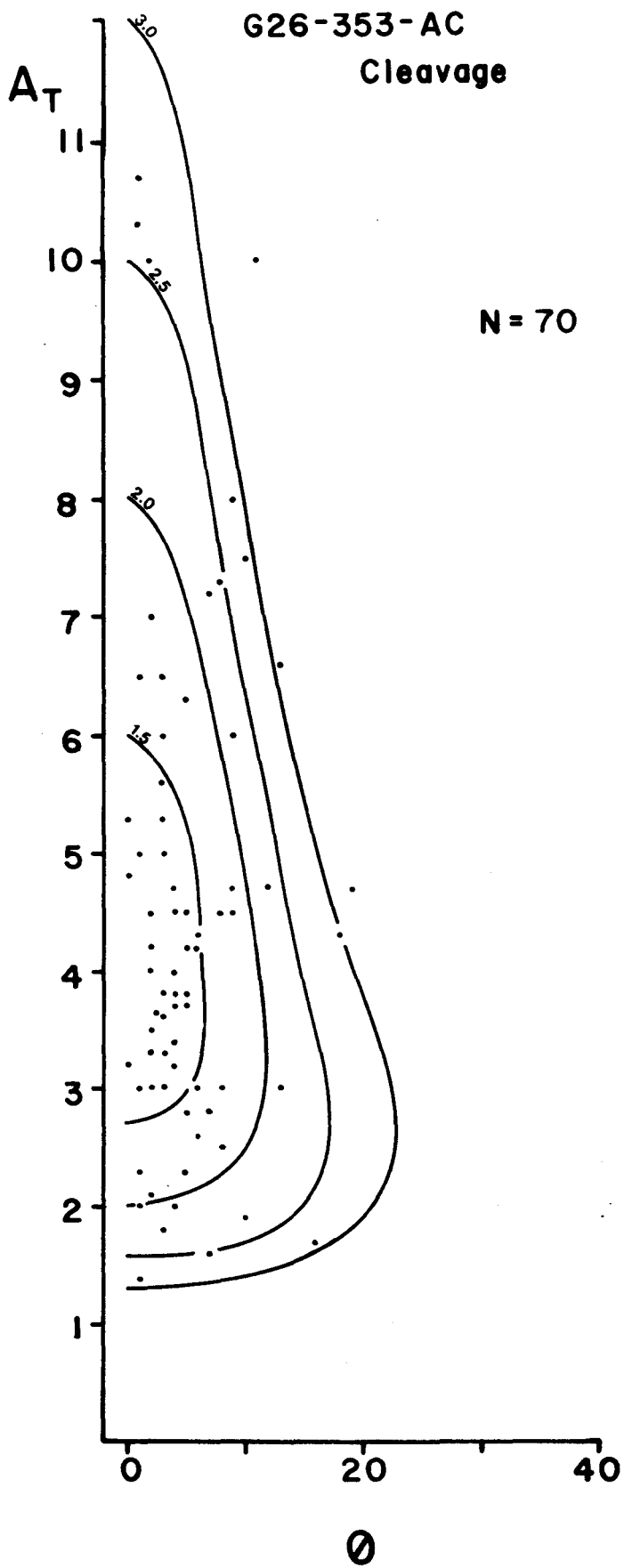
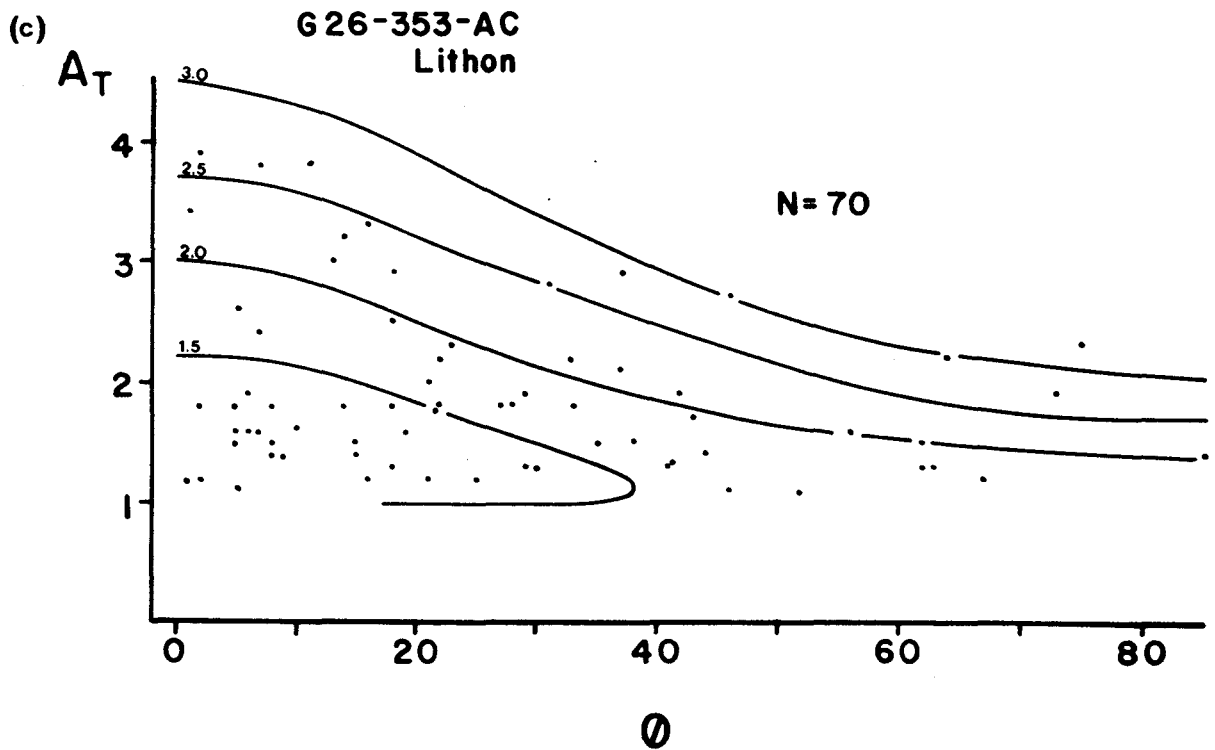
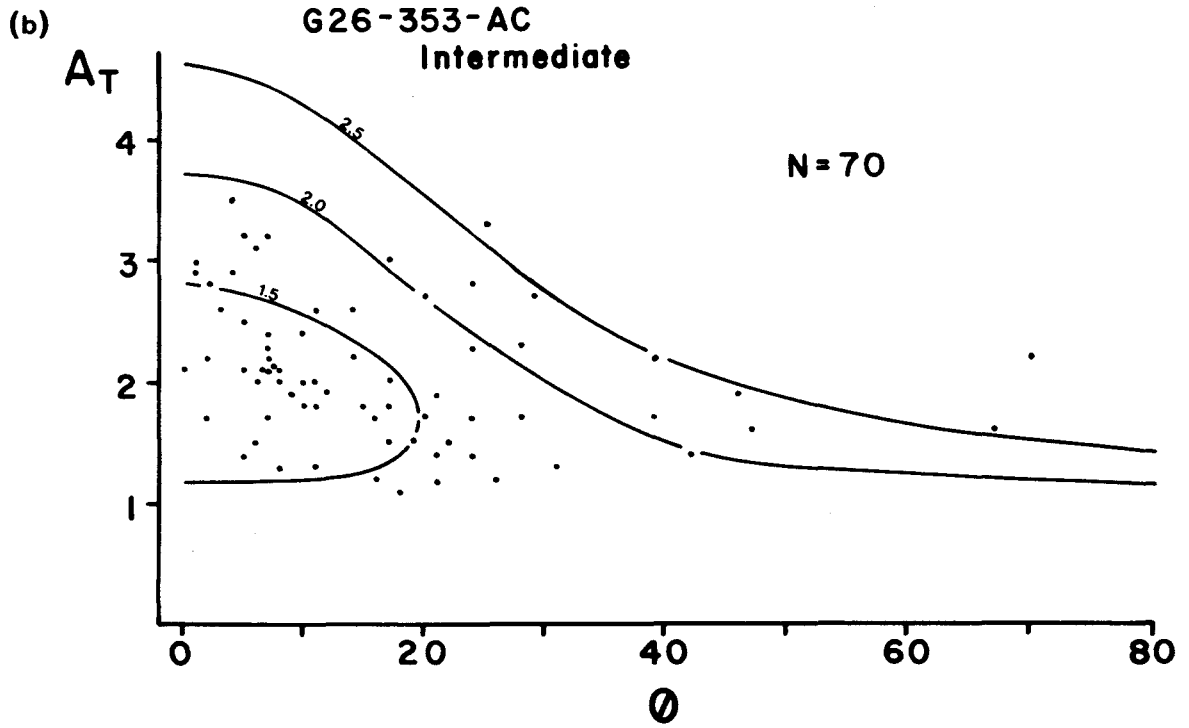


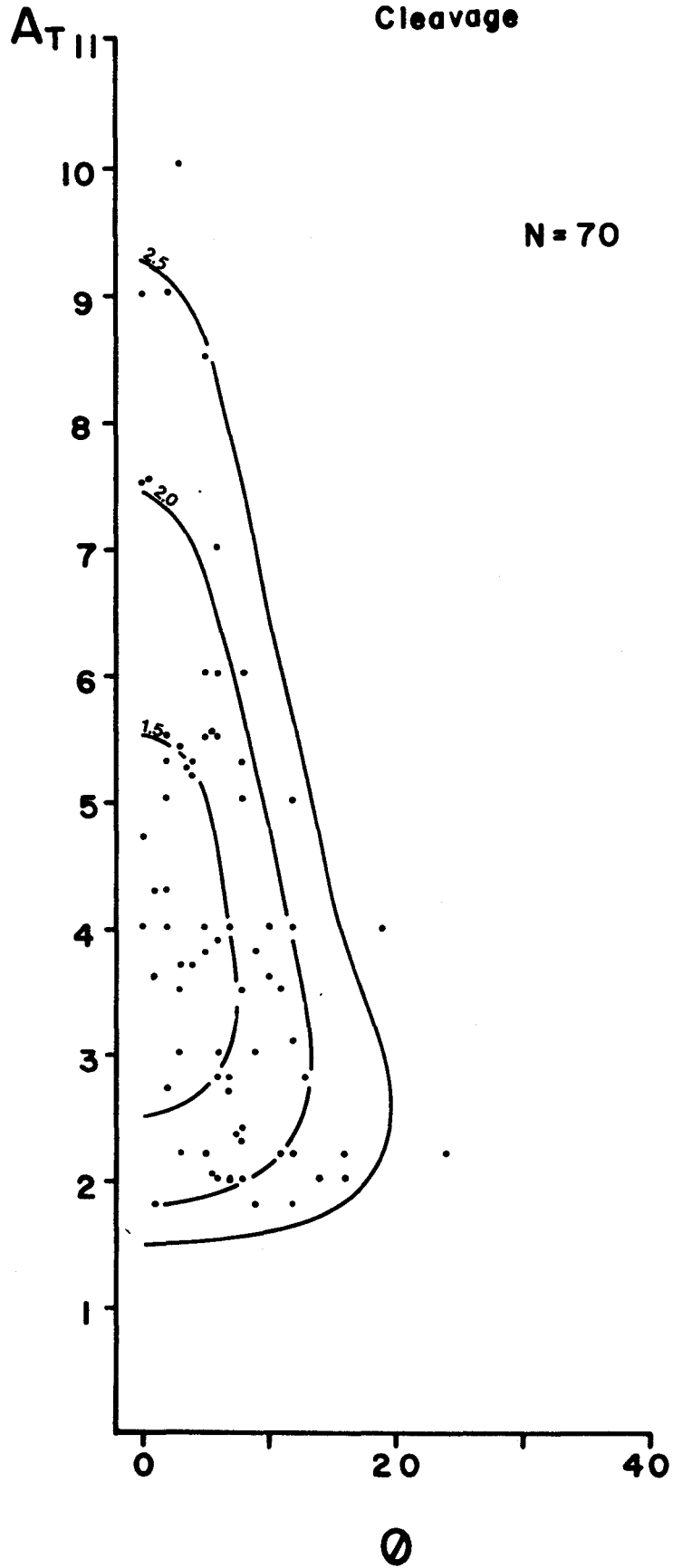
Figure 2.2.2a-f Scatter diagrams for slide G26-353

(a)





(d)

G26-353-BC
Cleavage

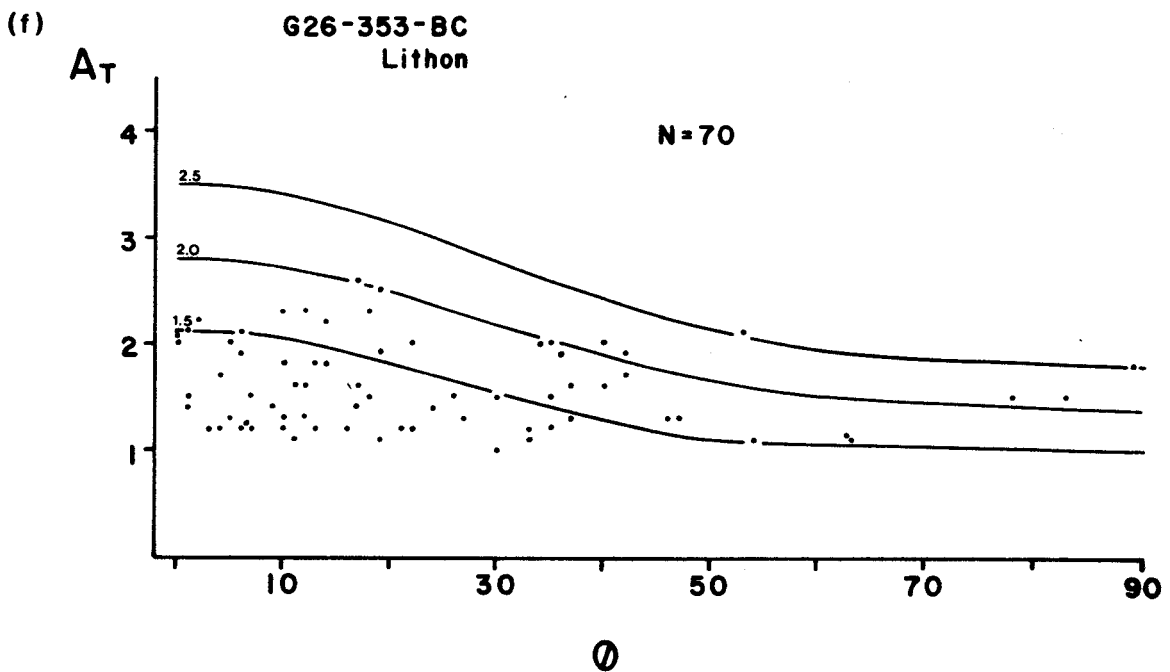
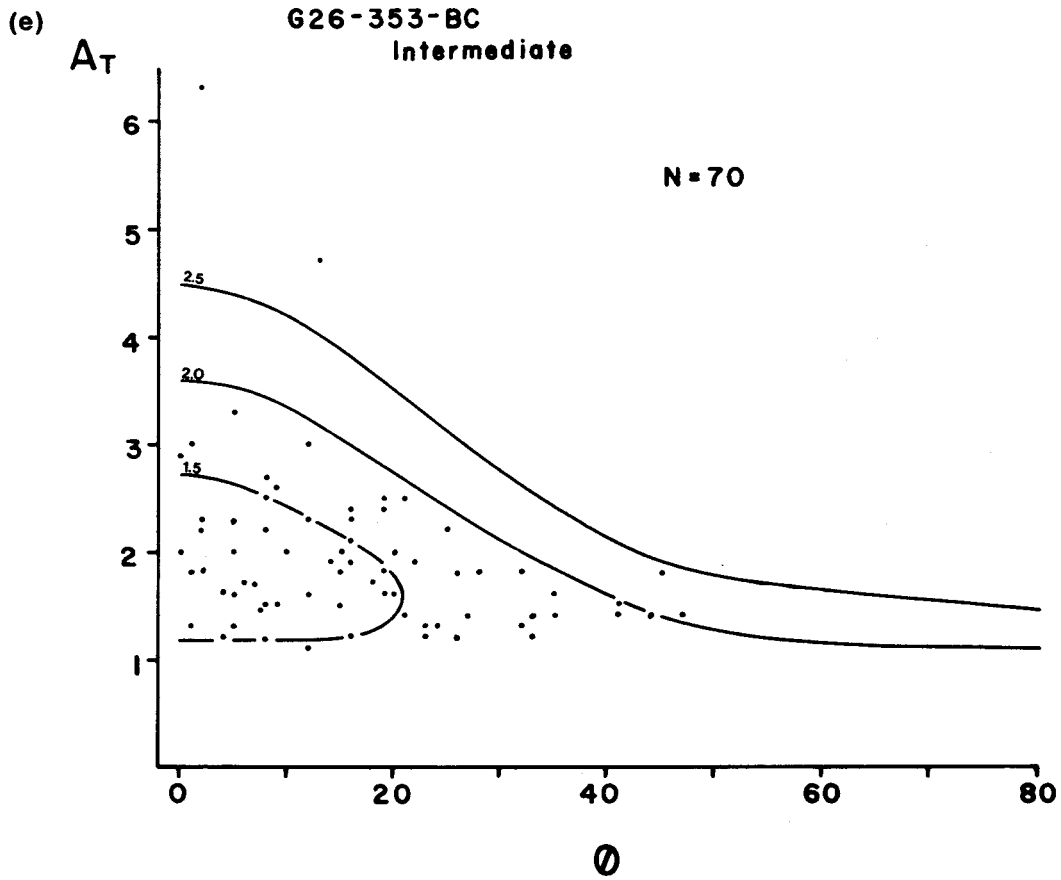
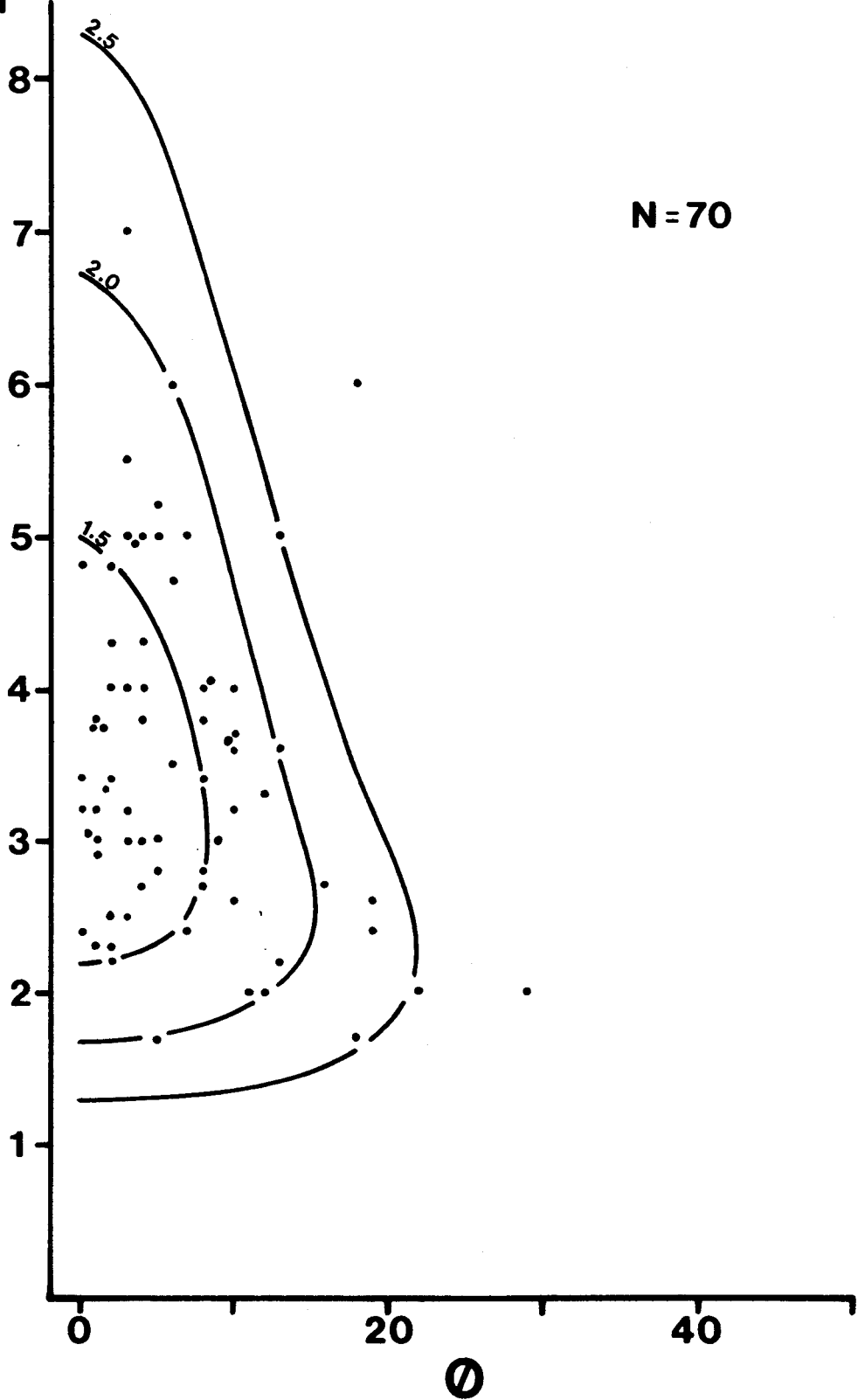
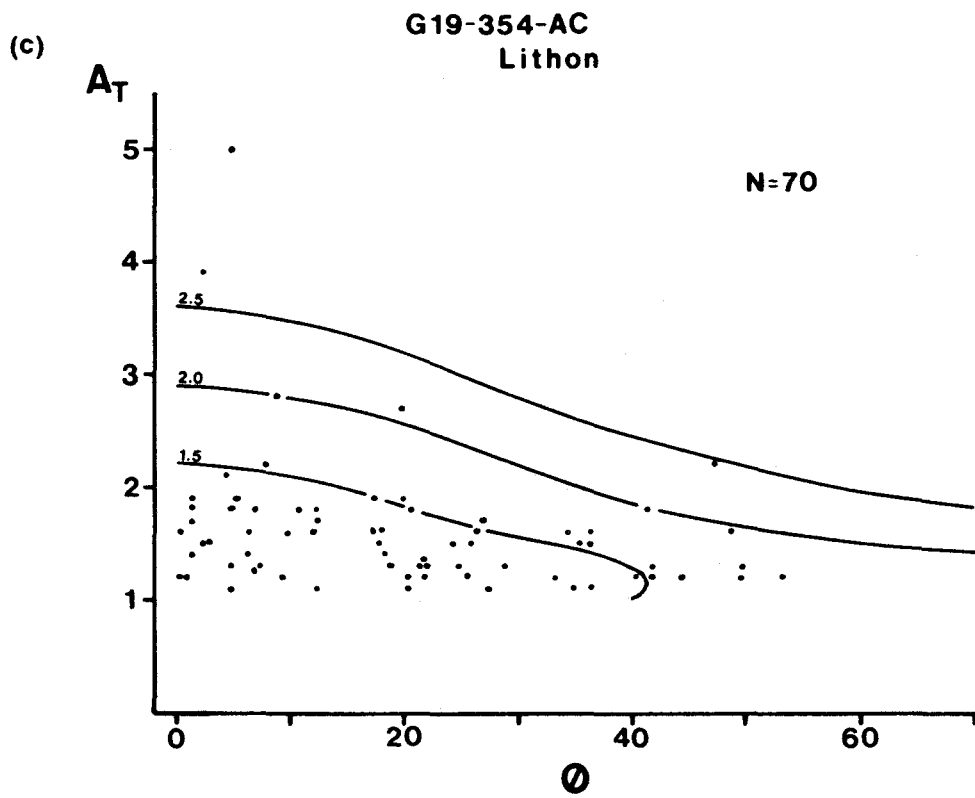
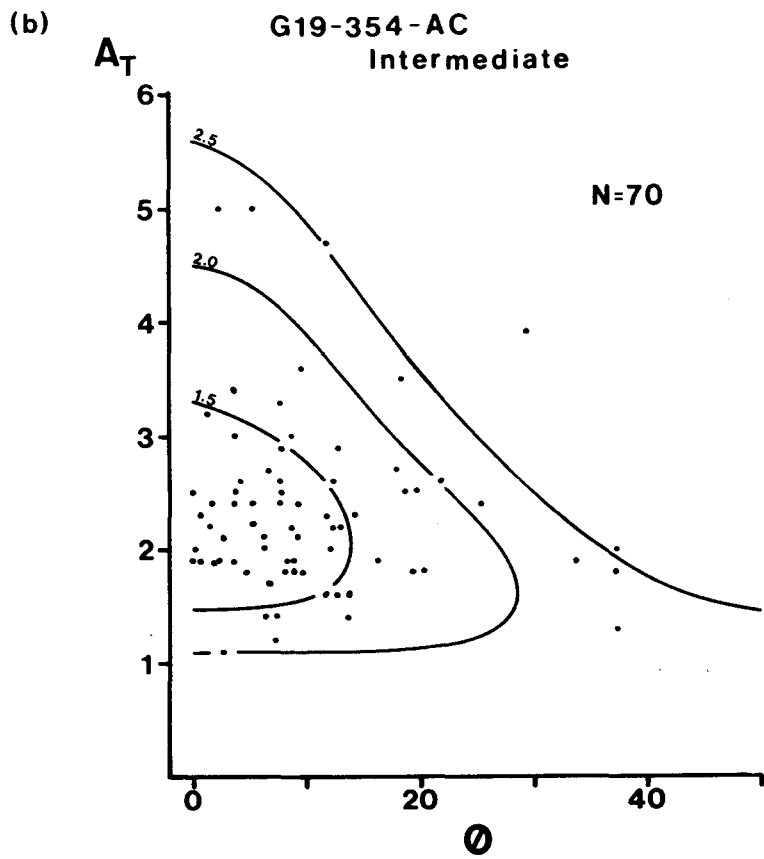


Figure 2.2.3a-f Scatter diagrams for slide G19-354

**G19-354-AC
Cleavage**

(a)

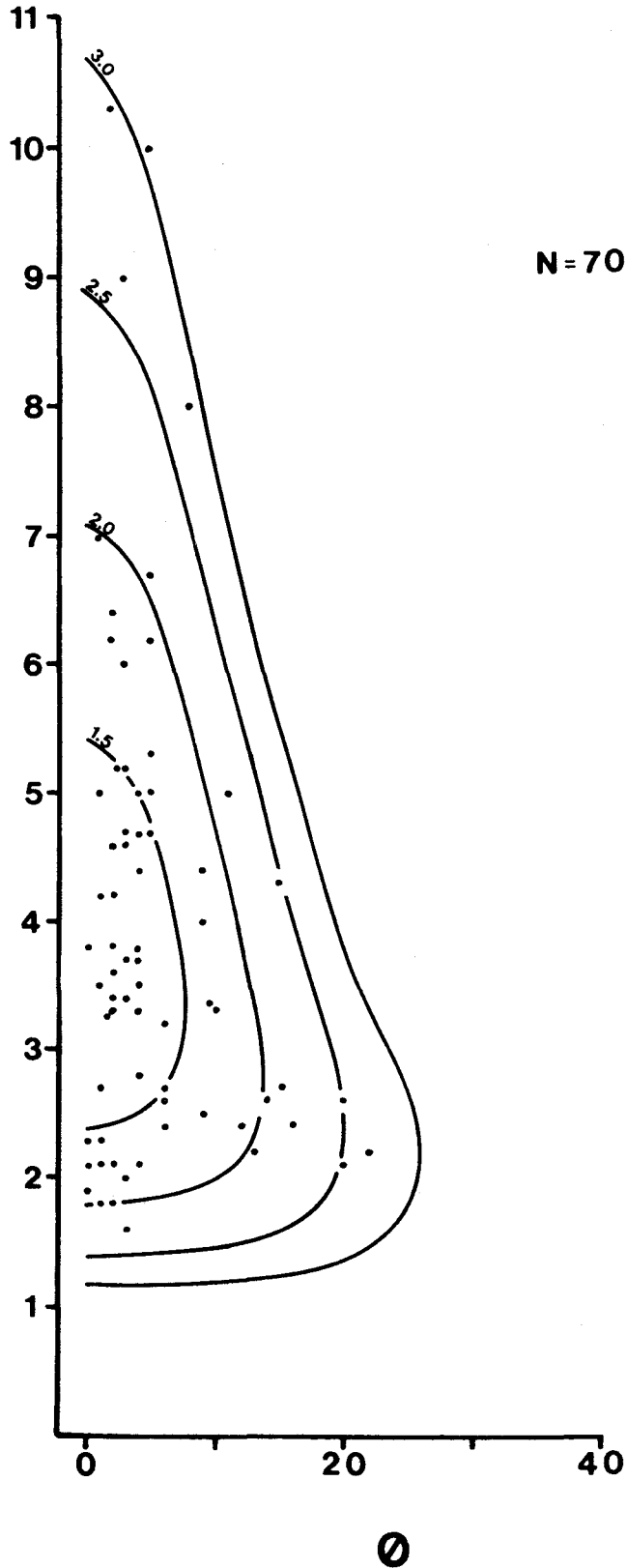
 A_T 



G19-354-BC
Cleavage

(d)

A_T



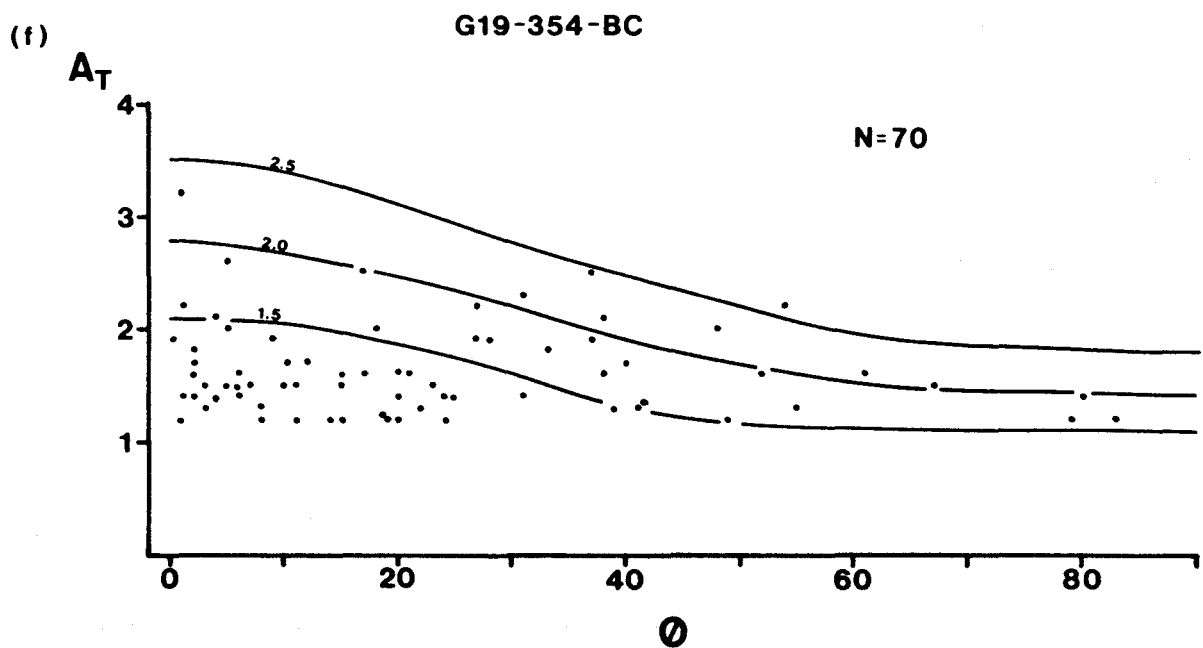
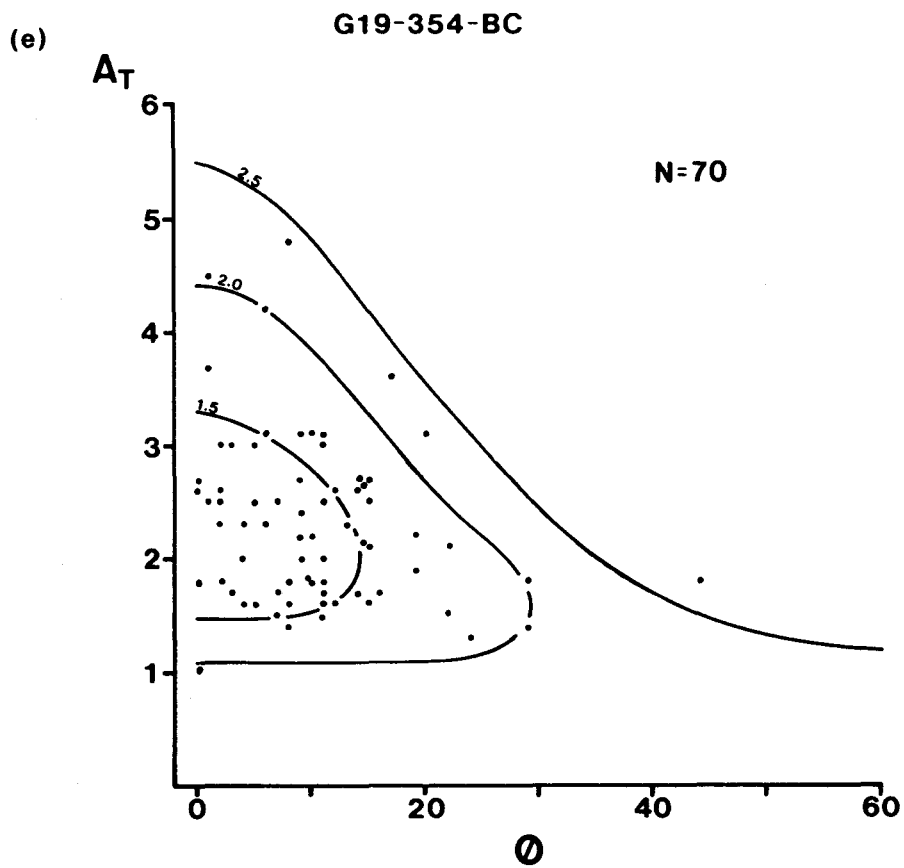


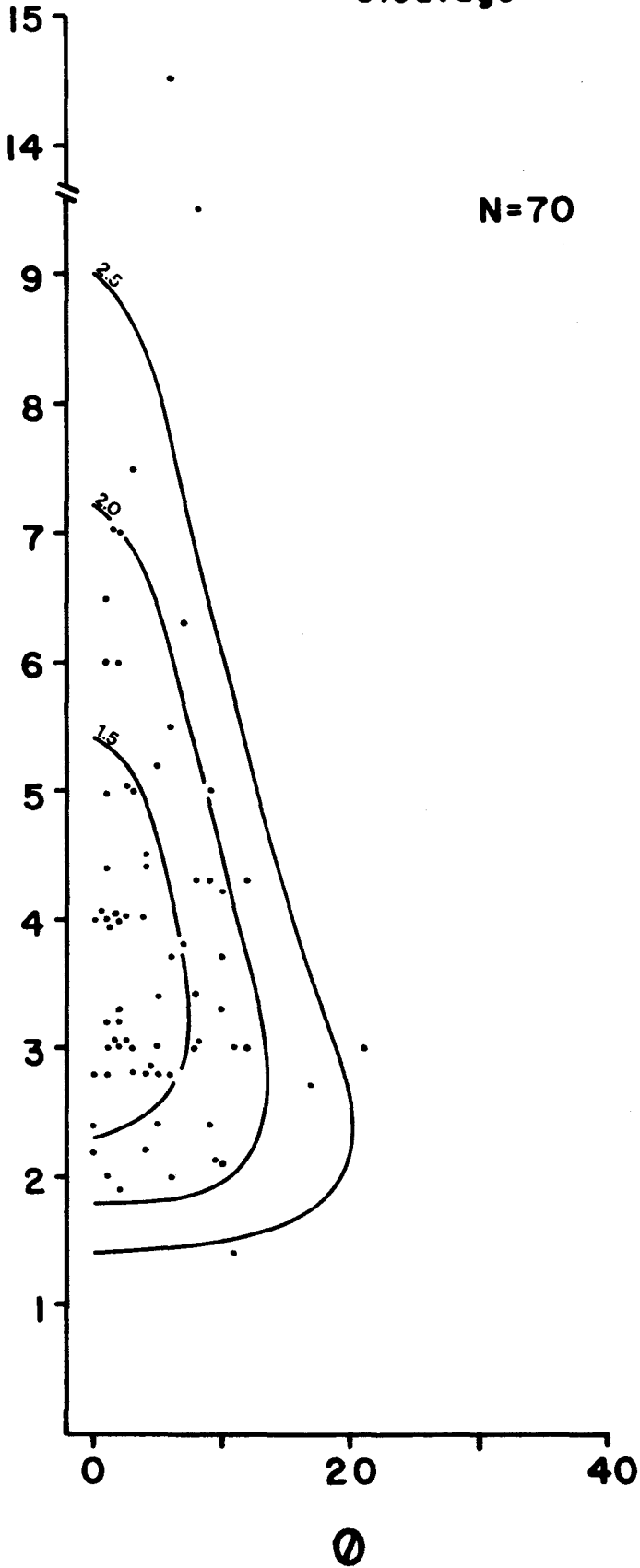
Figure 2.2.4a-c Scatter diagrams for slide G20-747

(a)

G20-747-AC
Cleavage

A_T

N=70



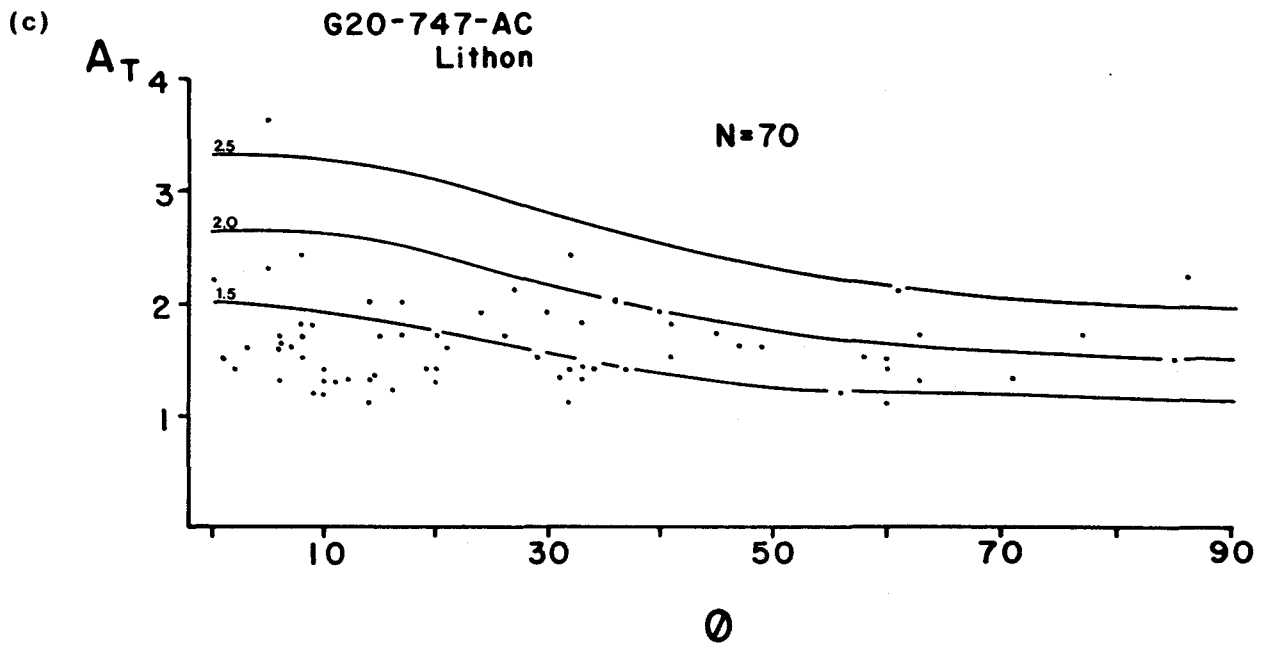
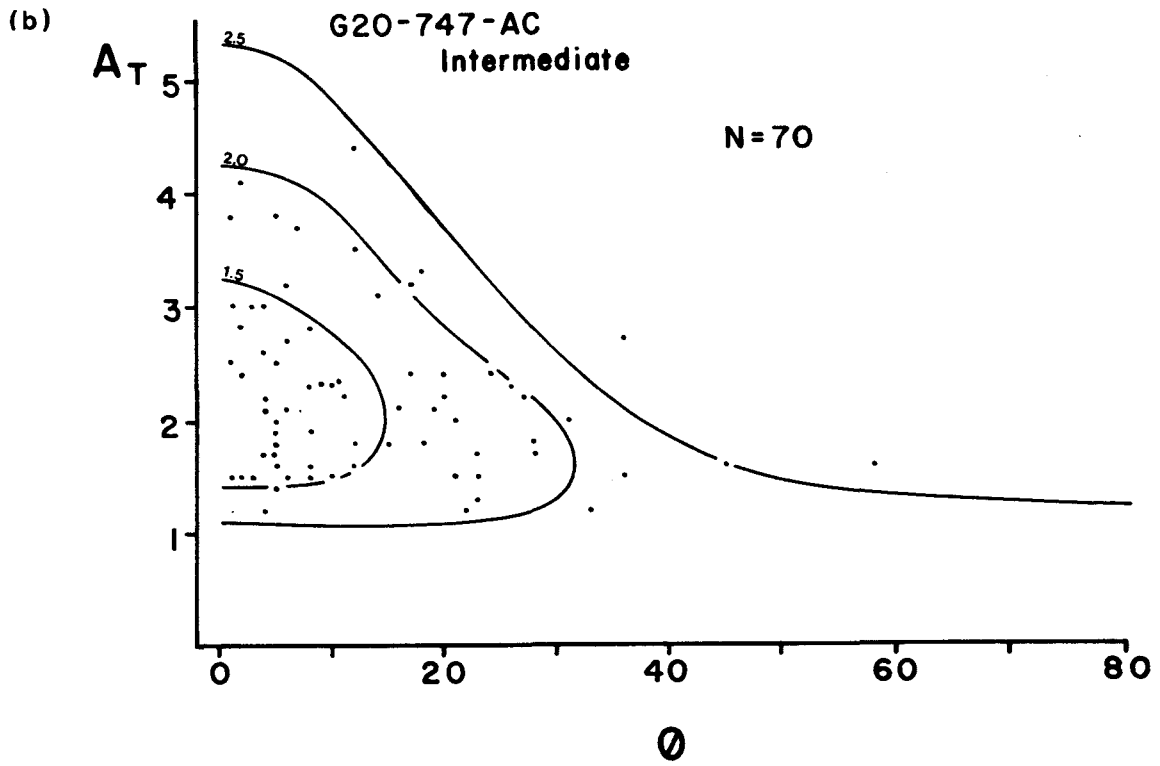
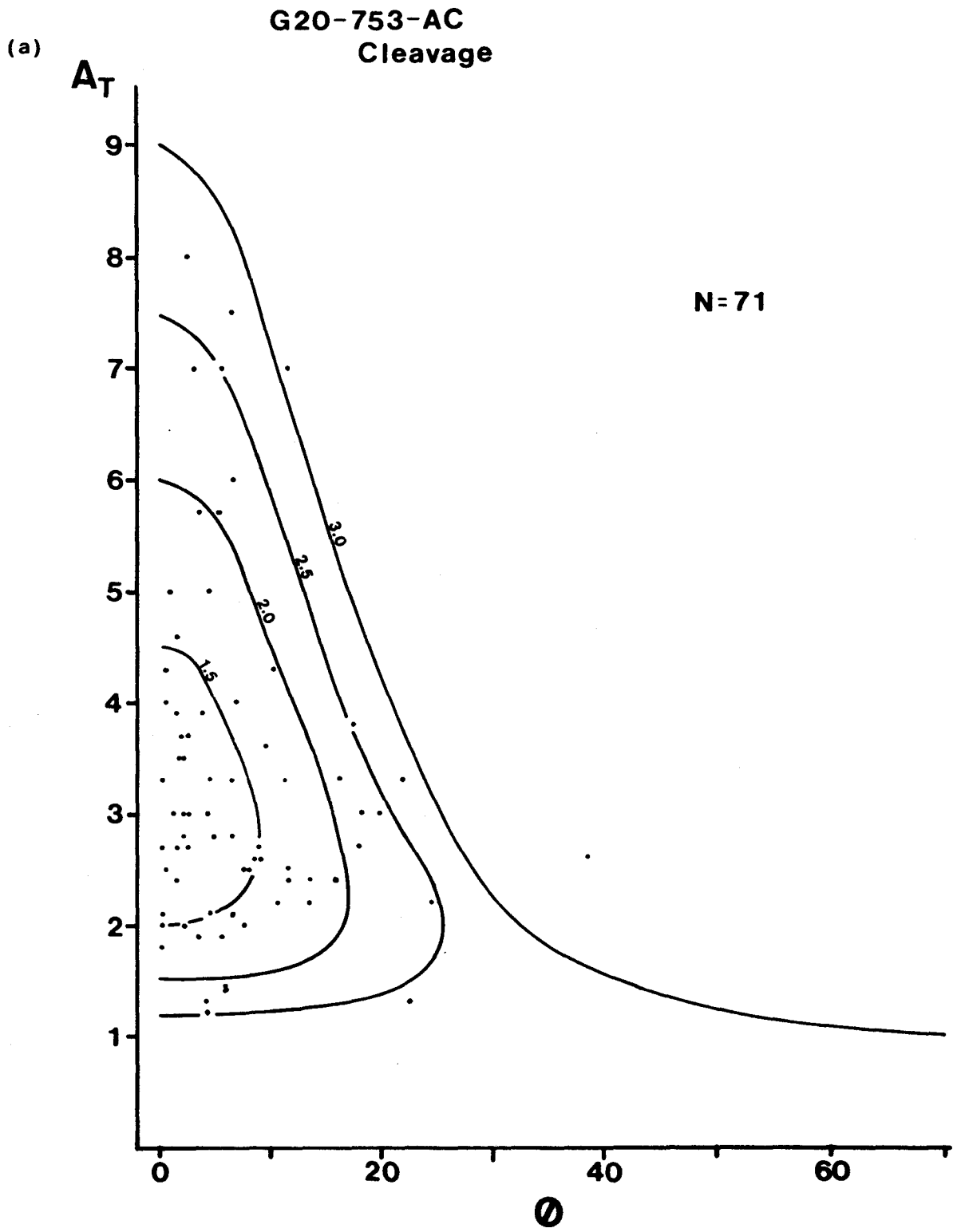
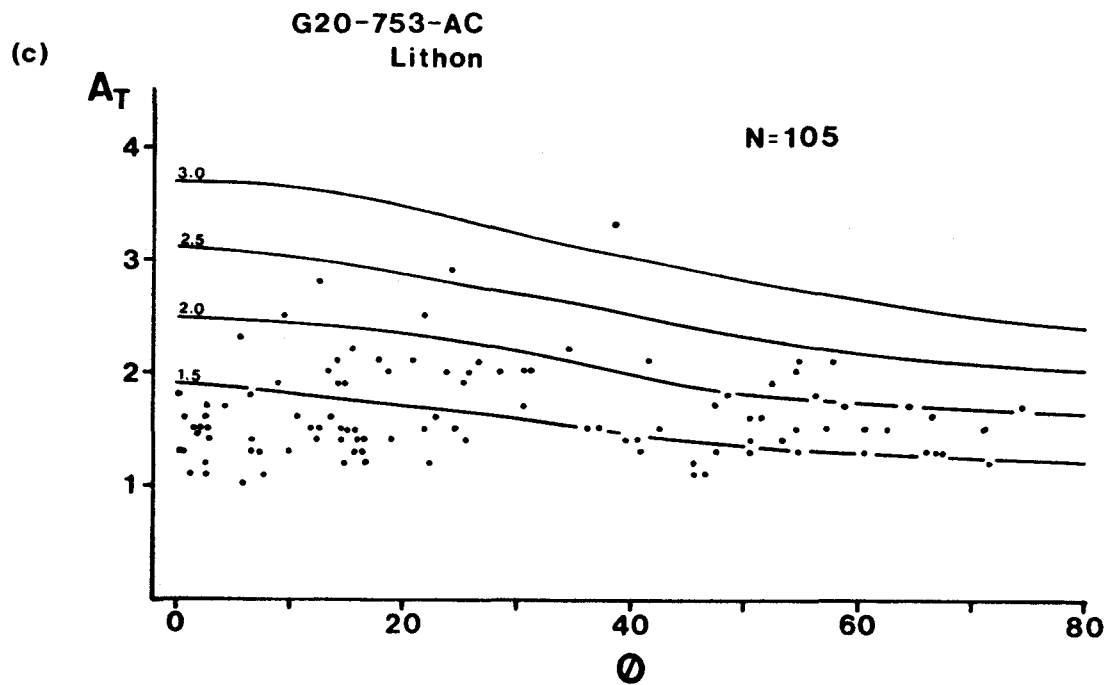
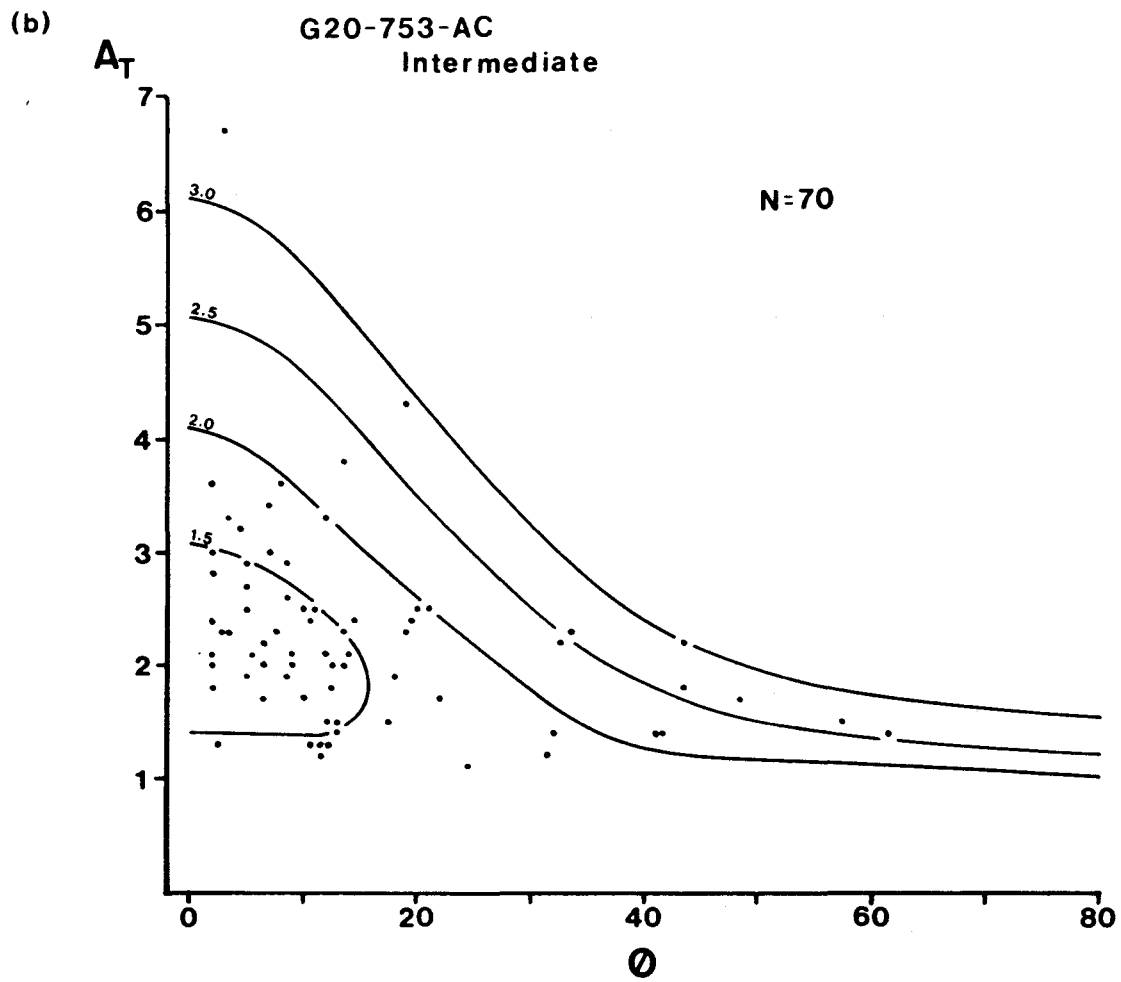


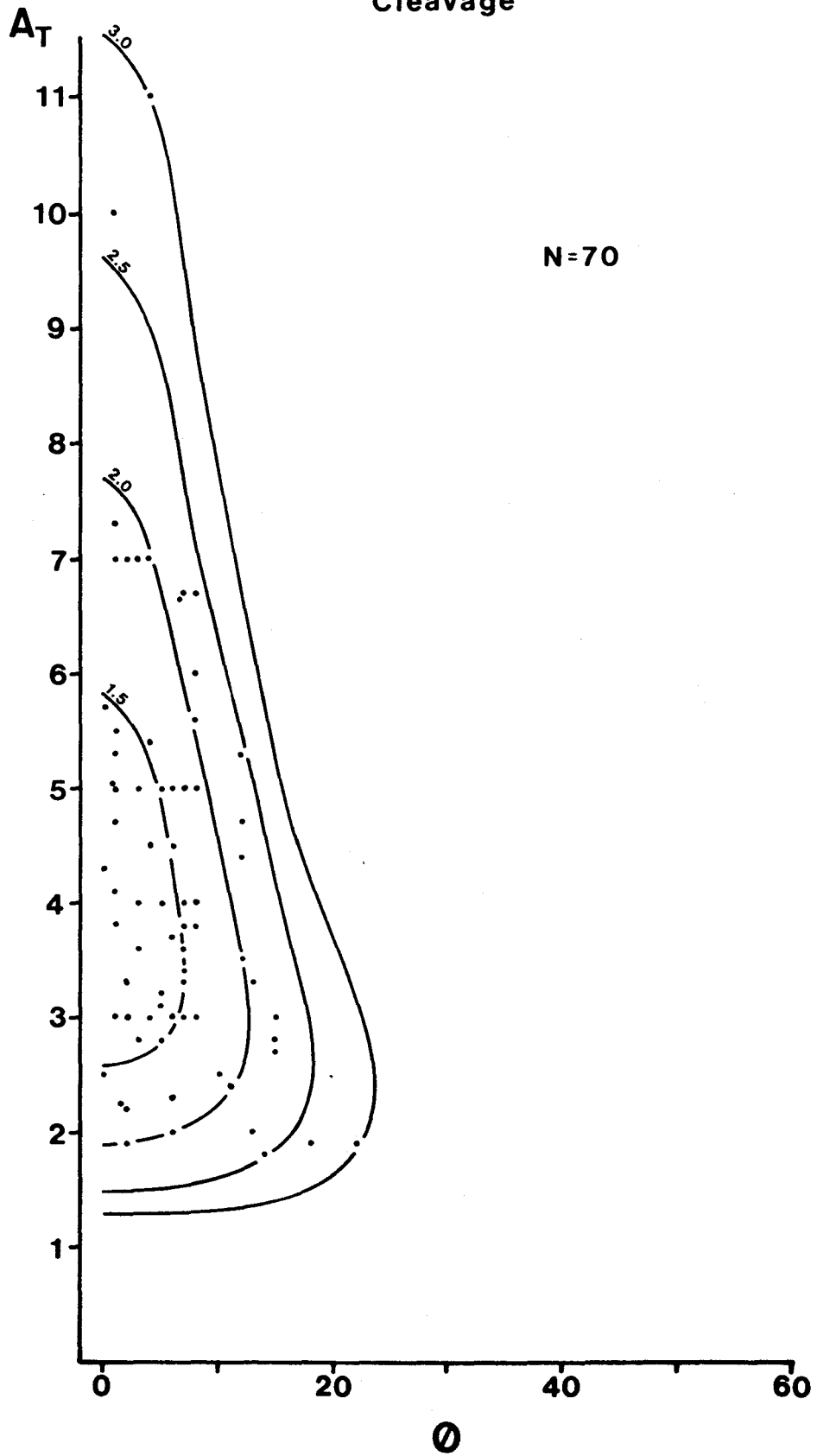
Figure 2.2.5a-f Scatter diagrams for slide G20-753

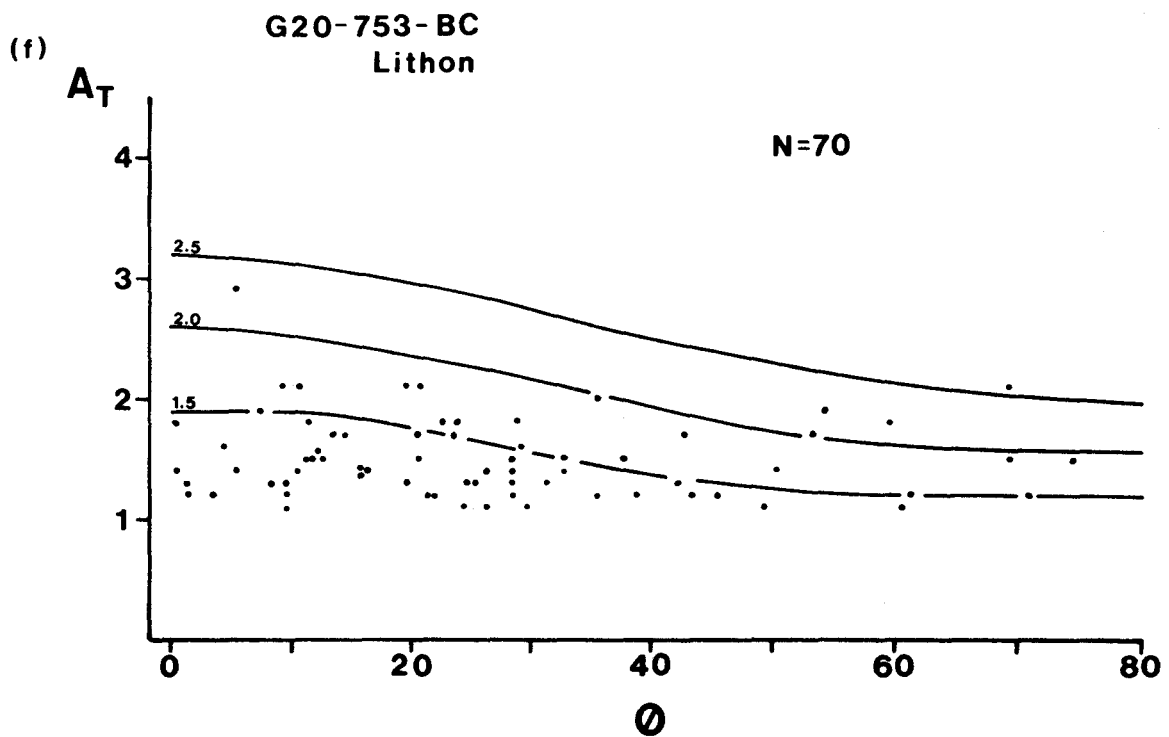
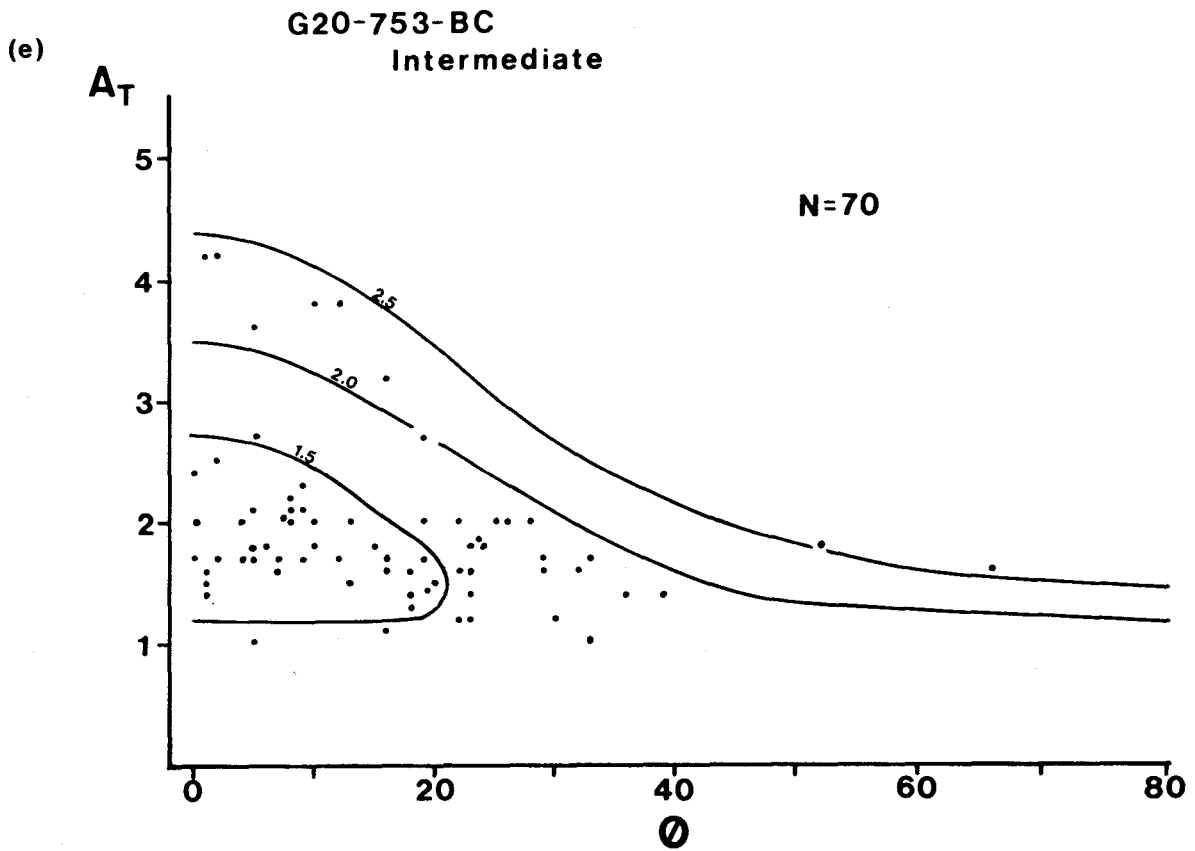




G20-753-BC
Cleavage

(d)





2.3 Deformation Plot

Measurements so far indicate that these samples have an oblate deformation ellipsoid ($1 > K > 0$, Ramsay 1967). Strain ellipsoid shapes can be represented on a two dimensional deformation plot (Flinn, 1962) in which relative shape changes may be illustrated. The natural logarithms of the two ratios of the principal semi axis lengths are used, (Ramsay 1967, Dunnet 1969, Ramsay et al 1972) with $a = \ln(1+e_1/1+e_2)$ as the ordinate and $b = \ln(1+e_2/1+e_3)$ as the abscissa. On this plot the origin represents a sphere ($e_i = 0$). The degree of oblateness or prolateness is expressed in terms of the parameter $K = a/b$. The line $K=1$, having unit slope, separates the field of oblate and prolate ellipsoids. This line may also be considered to separate the field of "apparent constriction" ($K > 1$) from that of "apparent flattening" ($K < 1$) (Ramsay & Wood, 1972).

In the process of deformation an original sphere passes through a series of ellipsoid shapes until it reaches its finite deformation ellipsoid. This series of shape changes defines the deformation path.

The strain ellipsoid determined for each of the three areas in each sample are shown on a deformation plot (Figure 2.3.1). With only one exception, all points lie in the field

of "apparent flattening". In three of the four samples, the three points, cleavage, intermediate and lithon, from a single sample define a reasonably straight line originating from $K=0$ (the origin). Thus, the lithon, intermediate and cleavage areas appear to represent three stages in the progressive deformation of the rock.

The K values determined for each of the samples (neglecting the lithon and intermediate values in G26-415) range from $K=0.05$ to $K=0.2$. According to Ramsay and Wood (1972) the cleavage should become more perfectly developed as the K value decreases. This is partially true for these samples. The sample with the highest K value ($K=0.2$, G20-753) does have the poorest cleavage definition. For the other three samples, the K values fall between 0.05 and 0.1. The cleavage definition does not necessarily increase as K decreases. The range in K values for these three samples is so small that this difference may be attributed to error.

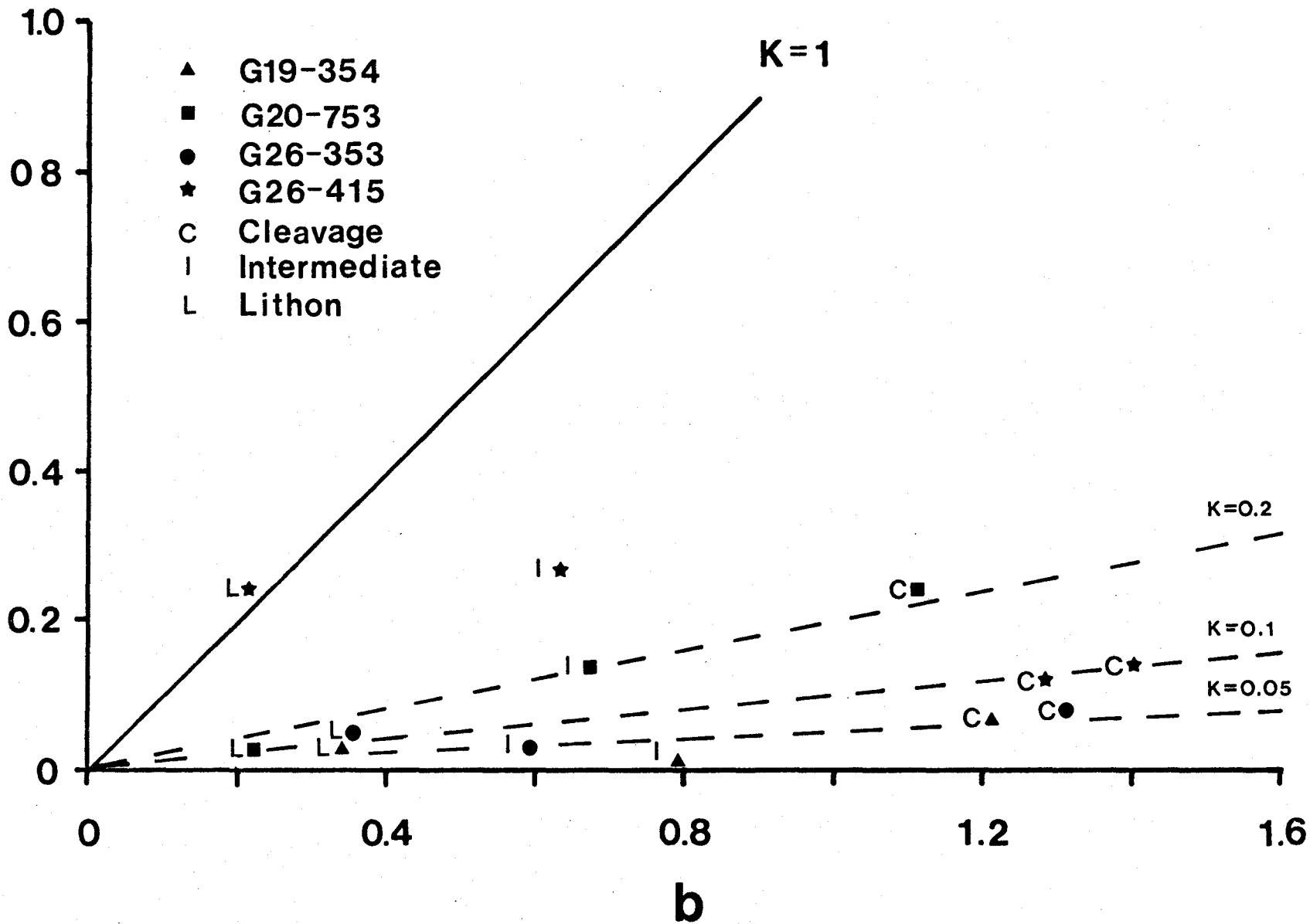
In the sample whose points do not fall on a line from the origin (G26-415) the lithon and intermediate points have a much higher value than would be expected, based on the behaviour of the other samples. This sample also has the best defined, widest cleavage, and the largest amount of recrystallized quartz in the lithon. In this case much more strain has occurred in the lithon, than in the other

lithons, the strain occurring largely by recrystallization of quartz, rather than simply by pressure solution. The cleavage strain ellipsoids for this sample fall within the general field of deformation of all the cleavage samples. So for the cleavage itself, the mechanism of deformation is consistent.

Figure 2.3.1 Deformation plot of Goldenville samples.

Dashed lines show possible deformation paths.

a



2.4 Volume Loss

Oblate deformation ellipsoids may develop in materials undergoing plane strain accompanied by a finite volume loss (Ramsay, 1967). Where volume change has occurred, the line separating the field of flattening from that of constriction is shifted upward (for volume gain) or downward (for volume loss). The slope remains at 45 degrees. "Total volume change per original unit volume (dilation Δ) can be expressed in terms of the principal logarithmic strains:

$$\ln(1+\Delta) = \epsilon_1 + \epsilon_2 + \epsilon_3" \quad (\text{Ramsay and Wood, 1972})$$

where $\epsilon = \ln(1+e)$

If the deformation path is a straight line with a slope less than unity, then there has been an incremental volume loss during deformation. Since the points of each sample essentially define a straight line in Figure 2.3.1, then such an incremental loss is inferred.

In the samples studied the "apparent flattening" process is produced by shortening along the Z-direction without a proportionate elongation in the X direction. This shortening has been achieved largely by pressure solution of quartz.

Figure 2.4.1 Deformation plot of Goldenville samples
showing the volume loss component.

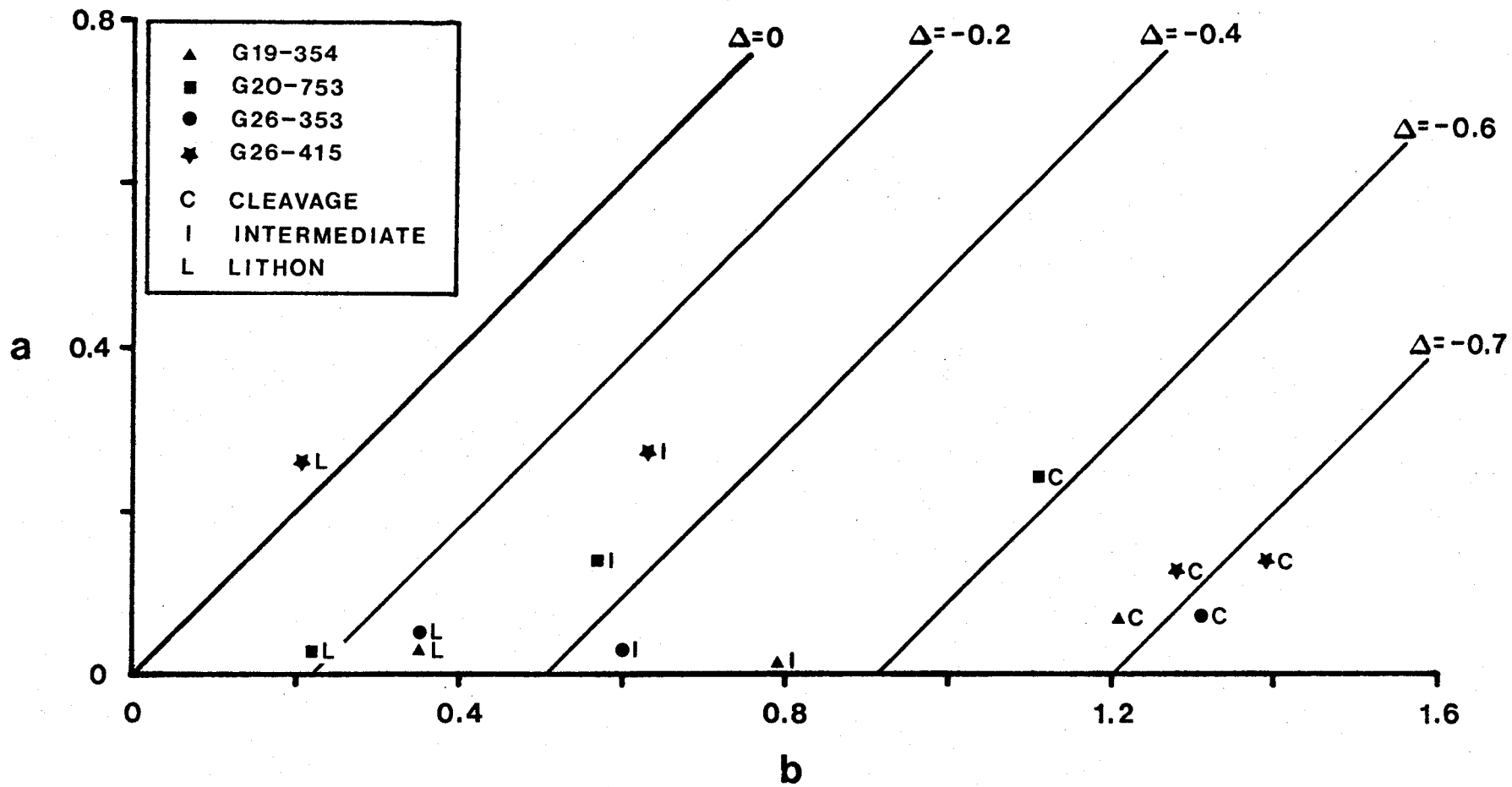


TABLE 2
Calculated Volume Loss

Sample	Δ	VL(PS)	Δ -VL(PS)	$\Delta_c - \Delta_L$
G26-415				
C	-0.71	-0.67	+0.04	-0.76
2C	-0.68	-0.64	+0.04	-0.73
I	-0.31			
L	+0.05			
G26-353				
C	-0.71	-0.62	+0.09	-0.45
I	-0.40			
L	-0.26			
G19-354				
C	-0.68	-0.59	+0.09	-0.41
I	-0.54			
L	-0.27			
G20-753		-0.63		
G20-753				
C	-0.58	-0.62	-0.04	-0.40
I	-0.36			
L	-0.18			

C Cleavage; I Intermediate; L Lithon.

Δ Ramsay-type volume loss.

VL(PS) Simple pressure solution volume loss.

The points have been plotted on a second deformation plot showing the location of the line $K=1$ for increasing amounts of volume loss (Figure 2.4.1). The volume loss for each set of measurements has been calculated using the aforementioned (Ramsay and Wood, 1972) expression for dilation. These values are shown in Table 2. The volume loss in all samples decreases from cleavage to lithon. The cleavage samples that have lost the greatest volume (71 percent) are those taken from the core of the anticline (G26-353 and G26-415). The cleavage which has lost the least volume is, not suprisingly, the sample taken the farthest down the limb (G20-753, 58 percent). Volume loss in the intermediate areas of each section range from 31 percent to 54 percent; in the lithons, values range from a 27 percent loss in volume to a 5 percent volume gain. The range in values in the cleavage (approximately 10 percent) is much smaller than that in either the lithon (approximately 30 percent) or the intermediate zones (approximately 25 percent). This again suggests that the mechanism responsible for cleavage formation acted similarly in all samples, with slight deviations occurring depending on the location of the sample within the anticline.

A second, crude, volume loss calculation was made using the ratio of the $A<t>$ value in the cleavage. The ratio ($A<t>$)

lithon/ A_{cleavage}) is equivalent to the fraction of a grain (having the original dimensions of the lithon strain ellipse) that remains after experiencing a one dimensional area loss, resulting in a ellipse equivalent to that found in the cleavage. Thus:

$$\left(\frac{A_{\text{lithon}}}{A_{\text{cleavage}}} - 1\right) \times 100 = \text{percent area loss}$$

The calculation has been done in each ac and bc section and the two values have been averaged to give a cleavage volume loss. The results of this calculation are also shown in Table 2. This type of volume loss calculation has many inherent assumptions. It assumes that:

1) the lithons are representative of the original rock prior to deformation.

2) the volume loss was in one dimension only (the Z principal axis) with no associated plastic deformation, i.e. the change in axial ratio is due solely to a unidirectional volume loss.

3) the loss of volume is due solely to a loss of quartz. Some of these assumptions are obviously incorrect. For example, the lithons have undergone some deformation, clearly shown in their loss of volume.

Comparison of Ramsay type volume loss and the pure

pressure solution volume loss, (volume loss difference in Table 2), shows the results to be remarkably similar. All values fall within less than 10 percent of each other. In three out of the four cases where this comparison could be made, that determined using the pure pressure solution model was lower than the Ramsay value. The sample for which this was not the case was that which was located farthest down the limb (G20-753). This difference in volume is due to some of the strain being taken up in axes other than the Z principal axis. The difference between this and other samples can be seen in the deformation plot (Figure 2.3.1)

The similarity in the results from the two types of calculation illustrates that the change in shape of grains from lithon to cleavage is due mainly to a loss of quartz via pressure solution and this loss was accommodated in the Z direction.

The amount of volume lost in the lithons is surprisingly high. This is possibly due to compaction before the process of cleavage formation began. During the initial compaction process, elongate grains may have reoriented themselves, resulting in a loss of pore space and its associated fluid. The amount of volume lost in this process could be anywhere from zero to the final value determined. All parts of the rock would have undergone this initial compaction, so it

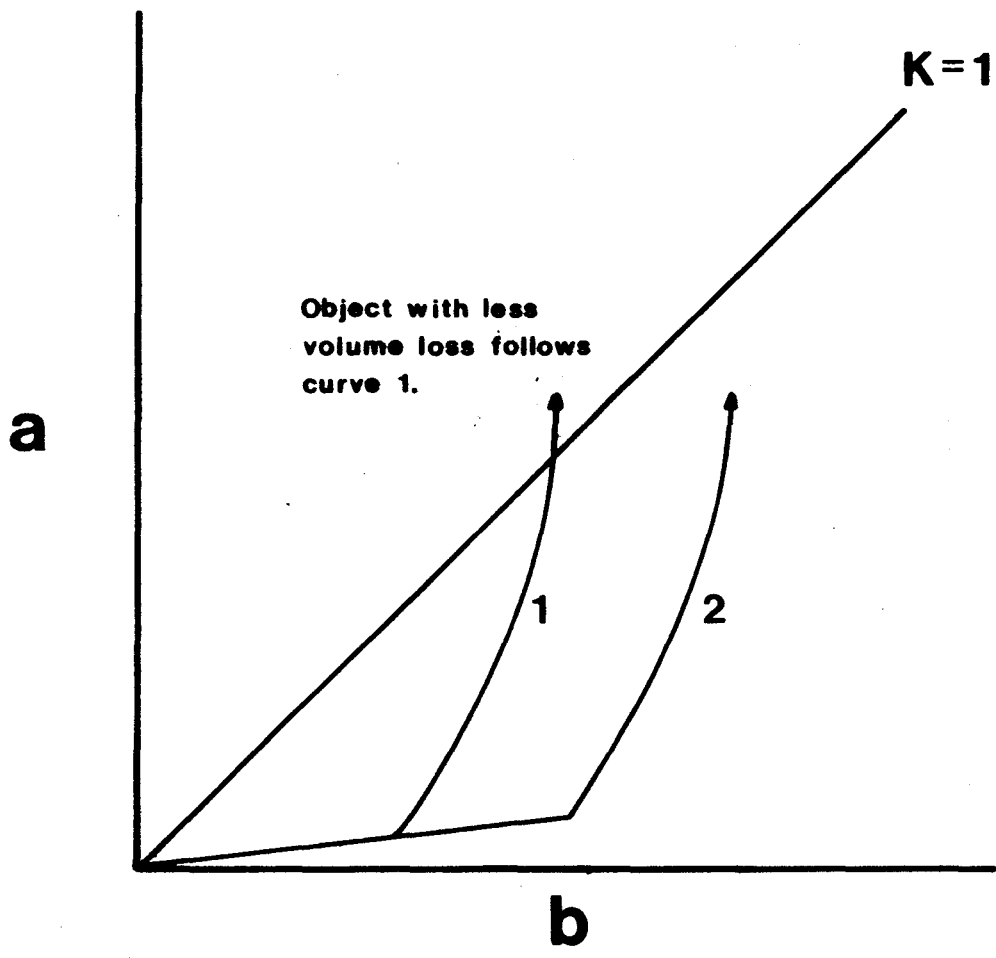
applies to cleavage and intermediate areas as well.

Assuming that all of the volume lost in the lithons is due to compaction, then the difference between cleavage and lithon values would represent the total volume of silica lost from cleavage zones. (Table 2, $\Delta_c - \Delta_L$). In all cases, this quantity is 40 percent or greater. These values agree closely to the volume losses determined by chemical and modal analyses (Fueten et al, in press).

The volume gain in lithon G26-415 appears to be unusual. If the entire system had undergone an initial compaction by loss of pore space, this section would be expected to behave like the others. The apparent gain in volume may be a result of a constrictive effect which occurred during folding. This would cause the deformation path to "move away from the field of apparent flattening toward the apparent constriction field." (Ramsay and Wood, 1972). The lower the amount of volume loss that occurs before constriction, the closer the final strain will be to the field of "apparent constriction". If cleavage formation occurred prior to folding then the amount of volume lost would vary from cleavage to lithon. Thus the lithon would have a smaller volume loss than the intermediate area, such that after constriction it will lie closer to the field of "apparent constriction", (Figure 2.4.2). Such is the case

with this sample. The quartz in the cleavage could have avoided constriction by being contained within a zone having a much higher mica content. These zones would behave differently under these conditions with much more of the strain being taken up in the mica than in the quartz grain.

Figure 2.4.2 Sketch of the change in deformation path
due to a change in the nature of the strain.



2.5 Strain Due to Plastic Deformation

If the strain due to volume loss is removed from each ellipsoid, the resultant ellipsoid should be that of the strain due to plastic deformation. The resultant strain values have been listed in Table 3. All the volume loss has been attributed to uniaxial pressure solution in the Z direction. Although this may often be the case, it is possible to shorten in the X and Y directions by the same process. This is accomplished where two grains, meet at some intermediate angle between Z and XY plane. Volume loss occurring at the grain boundaries may be resolved into an X (or Y) component and a Z component. The effect of this in the XY plane would be small, but in the situation where substantial volume loss has occurred, (as is the case in many of these samples), this effect should be measurable. The strain ratios listed in Table 3 should be considered as only one possibility for the strain ellipse due to plastic deformation. Also shown in Table 3 are the corresponding values for extension in the X direction and shortening in the Z direction. In most cases the strain due to plastic deformation is small compared to that due to volume loss. In the sample obtained from the core of the anticline (G26-415) this strain becomes substantial.

TABLE 3

Strain Due To Plastic Deformation

Sample	Strain Ratio	Extention in X	Shortening in Z
G26-415			
C	1.15:1:0.96	15%	4%
2C	1.13:1:0.96	13%	4%
I	1.31:1:0.84	31%	16%
L	1.30:1:0.79	30%	21%
G26-353			
C	1.15:1:0.98	15%	2%
I	1.03:1:0.96	3%	4%
L	1.05:1:0.96	5%	4%
G19-354			
C	1.07:1:0.98	7%	2%
I	1.01:1:0.99	1%	1%
L	1.03:1:0.98	3%	2%
G20-753			
C	1.27:1:0.91	27%	9%
I	1.15:1:0.92	15%	8%
L	1.03:1:0.98	3%	2%

C Cleavage; I Intermediate; L Lithon.

2.6 Bulk Strain Estimates

Estimates for the bulk strain have been calculated based on the percent cleavage in each sample. Since the boundaries of the cleavage zones are often diffuse, and grade into intermediate areas, the exact proportion of cleavage, intermediate and lithon areas could not be determined. On the average the cleavage accounted for 30 percent of the rock as a whole.

The bulk strain ratios are:

Sample	Strain Ratios	Bulk Volume Loss
G20-753	1.08:1:0.71	23%
G19-354	1.04:1:0.59	38%
G26-353	1.06:1:0.57	39%
G26-415	1.24:1:0.62	23%

These values give an overall X/Z strain ratio of 1.8. This value is similar to that determined by Henderson (1983) on the basis of aspect ratios of sand volcanoes found on bedding surfaces. Therefore the bulk strain estimates determined here appear to be reasonable

Volume losses calculated from the bulk strain values

range from 20 percent to 40 percent. These values should be considered a maximum for the system as a whole. Since much of this volume loss may be attributed to loss of pore space an estimate for the minimum amount of volume loss can be determined using the volume loss difference between corresponding cleavage and lithon. The results of these calculations are:

Sample	Bulk Volume Loss Due to Pressure Solution in the Cleavage
G20-753	8%
G19-354	12%
G26-353	14%
G26-415	24%

These values correspond to the loss of volume due to the cleavage forming process. They also reflect how well developed the cleavage is in the corresponding sample.

Sample G26-415 is the only sample showing a substantial extension in the principle X direction. Since this sample is derived from the core of the anticline, this behaviour is to be expected and supports the idea that much of the strain in this sample may be due to constriction.

2.7 Discussion

The number of recent studies in which a quantitative determination of volume loss has been done are limited. Few of these studies separate the strain into two components; strain due to pressure solution and strain due to plastic deformation.

Mitra (1978) has determined the finite strain which has occurred in the South Mountain Anticline. The geometric mean of his values gives a bulk strain ratio of 1.2:1:0.4. This value is somewhat higher than that determined for the Goldenville Anticline but the relationship between principal strain axes is similar. In this study the total strain was separated into strain due to pressure solution and strain due to "dislocation creep". The axial ratio of the pressure solution strain ellipsoid was determined using the area ratio of quartz in pressure shadows to the whole rock in both ac and bc principal sections. This method could not be applied to the Goldenville samples since the development of pressure shadows is limited and it appears that the majority of pressure dissolved quartz has been removed from the greywacke beds. Mitra determined the strain due to dislocation creep using deformed microscopic rutile needles within quartz grains. In the Goldenville samples, any rutile

needles found had suffered no apparent deformation so this method could not be applied either. The results of Mitra's study show pressure solution to be responsible for the majority of the total finite strain. Although the methods used here are different, the results are similar.

Lisle (1977) measured clastic grain shape and orientation for the Aberystwyth Grits, Wales. The cleavage in the samples studied was not as well developed as that in the Goldenville samples. Strain values determined by Lisle are comparable to lithon and intermediate values determined here, which is to be expected based on cleavage development. Strain was not quantitatively separated to give a pressure solution component.

Onasch (1983) has determined that, in the Martinsburg Formation, cleavage formation is responsible for a shortening of 29 to 55 percent normal to the cleavage. The greywackes, from which the measurements were taken, were deposited by turbidity current and are mildly deformed. "Pressure solution was the dominant mechanism during cleavage development" (Onasch, 1983). Strain ratios and shortening normal to cleavage were determined from detrital grain shape. Cleavage development was roughly equivalent to the poorest cleavage seen in the Goldenville samples. Strain values determined are again similar to lithon and

intermediate values determined here. It appears that the shortening determined for the Goldenville Anticline is reasonable.

Comparison of the strain values determined here for the Goldenville anticline, and values determined by other authors, shows that a large amount of shortening can and does occur during cleavage formation, and a large portion of this strain is accomplished by pressure solution of quartz grains.

CHAPTER 3

Conclusions

Based on calculations of strain in three morphologically different areas within a sample possessing a well defined cleavage, it has been demonstrated that strain ratios are not homogeneous on a centimeter scale. Within one distinct area, comparison of grain shape shows the strain to be homogeneous on a millimeter scale. The strain increases progressively from mid-lithon to cleavage areas. Both lithon and intermediate areas may be considered to represent the nature of early stages through which the cleavage has passed during its formation.

Samples which possess cleavage generally have an oblate deformation ellipsoid, a large amount of which can be attributed to loss of volume. A large proportion of the volume lost is due to pressure solution of detrital quartz grains dominantly in cleavage zones and, to a lesser extent,

intermediate zones.

The amount of strain due to plastic deformation is small compared to that due to volume loss. Exceptions to this arise when a large amount of recrystallization has occurred in the lithons.

Bulk strain estimates indicate that the total volume lost from the system as a whole is between 20 percent and 40 percent. Total volume loss due solely to cleavage formation ranges from 8 percent to 24 percent as cleavage development improves.

The overall strain ratio determined for the Goldenville Anticline is 1.1:1.0:0.6.

REFERENCES

- Beach, A. (1979). Pressure solution as a metamorphic process in deformed terrigenous sedimentary rocks. *Lithos*, 12, 51-58.
- Beach, A. (1982). Chemical processes in deformation at low metamorphic grades: pressure solution and hydraulic fracturing. *Episodes*, Vol. 1982, No. 4, 22-25.
- Dunnet, D. (1969). A technique of finite strain analysis using elliptical particles. *Tectonophysics*, 7, 117-136.
- Elliott, D. (1970). Determination of finite strain and initial shape from deformed elliptical objects. *Geol. Soc. Am. Bull.*, 81, 2221-2236.
- Flinn, D. (1962). On folding during three-dimensional progressive deformation. *Geol. Soc. Lond. Q. J.*, 118, 385-433.

- Fry, N. (1982). Metamorphic incongruent solution, diffusion and pressure solution stripes. *Lithos*, 15, 183-190.
- Fueten, F., Clifford, P.M., Pryer, L.L., Thompson, J. and Crocket, J.H. (in press). Distribution and localization of gold in Meguma Group rocks, Nova Scotia. Part III -- Shortening and cleavage production, and widespread mass removal of SiO₂.
- Griffiths, J.C. (1967). Scientific Method in Analysis of Sediments. McGraw-Hill, New-York, 508p.
- Henderson, J.R. (1983). Analysis of structure as a factor controlling gold mineralization in Nova Scotia. *Geol. Surv. Can. Paper 83-1B*, 13-21.
- Hsu, M. (1971). Analysis of strain, shape and orientation of the deformed pebbles in the Seine River area, Ontario. Unpublished Ph.D. Thesis, McMaster University, 179p.

- Lisle, R.J. (1977). Clastic grain shape and orientation in relation to cleavage from the Aberystwyth Grits, Wales. *Tectonophysics*, 39, 381-395.
- Mitra, S. (1978). Microscopic deformation mechanisms and flow laws in quartzites within the South Mountain Anticline. *Jour. Geol.*, 86, 129-152.
- Onasch, C.M. (1983). Origin and significance of microstructures in sandstones of the Martinsburg Formation, Maryland. *Am. Jour. Science*, 283, 936-966.
- Phinney, W.C. (1961). Possible turbidity-current deposit in Nova Scotia. *Bull. Geol. Soc. Am.*, 72, 1453-1454.
- Poole, W.H. (1971). Graptolites, copper and K-Ar in Goldenville Formation, Nova Scotia. *Geol. Surv. Can. Paper 71-1A*, 9-11.

Ramsay, J.G. (1967). Folding and Fracturing of Rocks.
McGraw-Hill, New York, 568p.

Ramsay, J.G. and Wood, D.S. (1973). The geometric
effects of volume change during deformation
processes. *Tectonophysics*, 16, 263-277.

Schenk, P.E. (1970). Regional variation of the
Flysh-like Meguma Group (Lower Paleozoic)
of Nova Scotia, compared to recent
sedimentation off the Scotian Shelf. *Geol.*
Assoc. Can., Spec. Paper 7, 127-153.

Sorby, H.C. (1863). Uber Kalkstein-Geschiebe mit
Eindrucken. *Jahrbuch F. Mineralogie*,
801-807. (Not seen).

Sorby, H.C. (1908). On the application of quantitative
methods to the study of the structure and
history of rocks. *Geol. Soc. Lond. Q.J.*, 64,
171-232.

Williams, P.F. (1972). Development of metamorphic
layering in cleavage in low grade
metamorphic rocks at Bergmagui, Australia.

Am. Jour. Sci., 272, 1-47.

Woodland, B.G. (1982). Gradational development of domainal slaty cleavage, its origin and relation to chlorite porphyroblasts in the Martinsburg Formation, Eastern Pennsylvania. *Tectonophysics*, 82, 89-124.